Environmentally-benign Conductive Polymer Passivating Coatings

WP SERDP SEED 2525

Naval Air Warfare Center Weapons Division

1900 N. Knox Road (Stop 6303)

China Lake, CA 93555-6106

PI: Dr. Peter Zarras

May 23, 2018

Final Report

REPORT DOCUMENTATION PAGE

Form Approved
OMB No. 0704-0188

1. REPORT DATE *(DD-MM-YYYY)*	2. REPORT TYPE	3. DATES COVERED *(From - To)*
05/23/2018	SERDP Final Report	

4. TITLE AND SUBTITLE
Environmentally-benign Conductive Polymer Passivating Coatings

5a. CONTRACT NUMBER

5b. GRANT NUMBER

5c. PROGRAM ELEMENT NUMBER

6. AUTHOR(S)
Dr. Peter Zarras

5d. PROJECT NUMBER
WP-2525

5e. TASK NUMBER

5f. WORK UNIT NUMBER

7. PERFORMING ORGANIZATION NAME(S) AND ADDRESS(ES)
Naval Air Warfare Center Weapons Division
1900 N. Knox Road (Stop 6303)
China Lake, CA 93555-6106

8. PERFORMING ORGANIZATION REPORT NUMBER
WP-2525

9. SPONSORING/MONITORING AGENCY NAME(S) AND ADDRESS(ES)
Strategic Environmental Research and Development Program
4800 Mark Center Drive, Suite 17D03
Alexandria, VA 22350-3605

10. SPONSOR/MONITOR'S ACRONYM(S)
SERDP

11. SPONSOR/MONITOR'S REPORT NUMBER(S)
WP-2525

12. DISTRIBUTION/AVAILABILITY STATEMENT
Distribution A; unlimited public release

13. SUPPLEMENTARY NOTES

14. ABSTRACT
Conductive Polymer (CPs) coatings were synthesized, characterized and coated onto Zn-Ni plated 4130 high-strength steel substrates (supplied by Wright Paterson Air Force Base (WPAFB)) by researchers at the Naval Air Warfare Center Weapons Division, China Lake, California. The evaluation of novel conductive polymer coatings developed by the Polymer Science & Engineering Branch of the NAWCWD was performed both by the NAWCWD Engineering Branch and the University of Dayton Research Institute (UDRI) Coatings Corrosion and Erosion Group. The coating samples that were supplied by the NAWCWD as part of the SEED/SERDP-supported research effort on developing environmentally-benign corrosion protective chromate-free coatings that offer low contact resistance on zinc-nickel electroplated steel substrates and can meet the requirements for use in military electrical connectors and assemblies. The project was coordinated by the NAWCWD and the Air Force Coatings, Corrosion & Erosion Laboratory (CCEL) with the goal of demonstrating the feasibility of this novel type of CP coating materials.

15. SUBJECT TERMS
American Society for Testing and Materials, Chemical polymerization, Conductive Polymer, Dry and Wet Tape Adhesion testing, Electrochemical Impedance Spectroscopy, Electrochemical polymerization, Energy Dispersive X-ray Spectroscopy, Hydrogen Embrittlement, Monomer synthesis, Neutral Salt Spray, Scanning electron microscopy

16. SECURITY CLASSIFICATION OF:			17. LIMITATION OF ABSTRACT	18. NUMBER OF PAGES	19a. NAME OF RESPONSIBLE PERSON
a. REPORT	b. ABSTRACT	c. THIS PAGE			Peter Zarras
					19b. TELEPHONE NUMBER *(Include area code)*
UNCLASS	UNCLASS	UNCLASS	UNCLASS	71	760-939-1396

1.0 Table of Contents

2.0 List of Tables

3.0 List of Figures

4.0 List of Acronyms

AF CCEL	Air Force Coatings, Corrosion & Erosion Laboratory
ASTM	American Society for Testing and Materials
BAM-PPV	Poly(2,5-bis(N-methyl-N-hexylamino)phenylene vinylene
^{o}C	Degrees Celsius
CP	Conductive Polymer
Cr(VI)	Hexavalent chromium
DMF	Dimethylformamide
DI water	Deionized water
EDS	Energy Dispersive X-ray Spectroscopy
EIS	Electrochemical Impedance Spectroscopy
EDOT	3,4-ethylenedioxythiophene compound
^{o}F	Degrees Fahrenheit
$FeCl_3$	Ferric Chloride
GC/MS	Gas Chromatography/Mass Spectrometry
HE	Hydrogen Embrittlement
ICP-AES	Inductively Coupled Plasma - Atomic Emission Spectrometer
1L	one layer
2L	two layers
LHE	Low Hydrogen Embrittlement
Mil	Thousandth of an inch
μm	micrometer
NAWCWD	Naval Air Warfare Center Weapons Division
$MgSO_4$	Magnesium sulfate
NMR	Nuclear Magnetic Resonance Spectroscopy
NSS	Neutral Salt Spray
NSF	Notched Fracture Strength
PANI	Polyaniline

PATTI	Pneumatic Adhesion Tensile Testing Instrument
SEM	Scanning Electron Microscopy
SERDP	Strategic Environmental Research and Development Program
TEA	Triethylamine
THF	Tetrahydrofuran
UDRI	University of Dayton Research Institute
V	Volts
WPAFB	Wright Paterson Air Force Base
Zn-Ni	Zinc- Nickel alloy

5.0 Keywords

American Society for Testing and Materials

Chemical polymerization

Conductive Polymer

diethyl ((2,3-dihydrothieno[3,4-*b*][1,4]dioxin-2-yl)methyl)phosphonate monomer

Dry and Wet Tape Adhesion testing

Electrochemical Impedance Spectroscopy

Electrochemical polymerization

Energy Dispersive X-ray Spectroscopy

Hydrogen Embrittlement

Monomer synthesis

Neutral Salt Spray

Pneumatic Adhesion Tensile Testing Instrument Testing

Poly[diethyl ((2,3-dihydrothieno[3,4-*b*][1,4]dioxin-2-yl)methyl)phosphonate]

Scanning electron microscopy

Zn-Ni coated high strength steels

6.0 Acknowledgements

The authors would like to gratefully acknowledge the financial support of the Strategic Environmental Research and Development Program (SERDP) SEED under the direction of Dr. Robin A. Nissan, Weapons Systems and Platform Manager.

The work completed under this program was a joint effort by researchers at the Naval Air Warfare Center Weapons Division, China Lake, California and Wright Paterson Air Force Base, Wright Paterson, Ohio.

Dr. Peter Zarras led the overall efforts of this SERDP SEED program and contributed to the synthesis and characterization of novel conductive polymers. Dr. John D. Stenger-Smith, Mr. Andrew Chafin and Engineering Scientist Development Program (ESDP) students - Ms. Shelley Vang, Mr. Todd Dames, Ms. Alicia H. Hughes and Mr. Jacob Letcher assisted in the synthesis and analysis of new monomers and intermediates leading to the development of novel CP compounds. In addition, the authors would like to thank Dr. Paul Goodman for the electropolymerization and electrochemical studies of these new compounds, film fabrication, contact resistance; Dr. Gregory Ostrom for iron analysis using ICP-AES; Dr. Lawrence Baldwin for the NMR analysis of intermediates, monomers and polymers and Ms. Roxanne Quintana for the GC/MS analysis of these compounds. Neutral salt spray, adhesion and spectroscopic/microscopy studies of the CP films coated Zn-Ni high strength steel panels were performed by Mr. James Amato and Ms. Monica Castañeda.

Ms. Diane Buhrmaster and Dr. Alexander Khramov led the WPAFB/UDRI team in the investigation of the CP coated Zn-Ni high strength steel panels for adhesion, neutral salt spray studies. Also, the film morphology of the coatings was studied by scanning electron microscopy, several additional coating samples were evaluated for hydrogen embrittlement and Mr. Matthew Rothgeb for preparing the WPAFB/UDRI draft report.

7.0 Abstract

Conductive Polymer (CPs) coatings were synthesized, characterized and coated onto Zn-Ni plated 4130 high-strength steel substrates (supplied by Wright Paterson Air Force Base (WPAFB)) by researchers at the Naval Air Warfare Center Weapons Division, China Lake, California. The evaluation of novel conductive polymer coatings developed by the Polymer Science & Engineering Branch of the NAWCWD was performed both by the NAWCWD Engineering Branch and the University of Dayton Research Institute (UDRI) Coatings Corrosion and Erosion Group. The coating samples that were supplied by the NAWCWD as part of the SEED/SERDP-supported research effort on developing environmentally-benign corrosion protective chromate-free coatings that offer low contact resistance on zinc-nickel electroplated steel substrates and can meet the requirements for use in military electrical connectors and assemblies. The project was coordinated by the NAWCWD and the Air Force Coatings, Corrosion & Erosion Laboratory (CCEL) with the goal of demonstrating the feasibility of this novel type of CP coating materials.

Two batches of the CP coating samples were tested for adhesion (including wet/dry tape adhesion and tensile PATTI adhesion), corrosion resistance properties via electrochemical impedance spectroscopy (EIS), a neutral salt spray exposure, and hydrogen embrittlement. EIS of coated Zn-Ni coated high strength steel and contact resistance of CP coatings before and after neutral salt fog experiments were determined. In addition to corrosion and adhesion properties testing, the morphology of the coatings was examined by scanning electron microscopy (SEM) and energy dispersive X-ray spectroscopy (EDS). Comparative evaluation of coating samples demonstrated reasonably good corrosion performance and strong adhesion to zinc-nickel electroplated steel substrate were achieved with the second batch of the coating samples when the coatings were applied in a two-layer fashion for a thicker buildup on Zn-Ni plated high-strength steel substrate.

These coatings showed no hydrogen embrittlement on 4340 high strength steel notched bars but did not meet the mil spec requirements for contact resistance before and after NSS. For these two-layer coating samples, the study of the film morphology revealed uniformly dense and defect-free coating.

This overall improvement in performance based on the second batch of coating samples brings these coating materials to a promising performance level that would justify further and more detailed investigation of these coatings.

8.0 Objective

The objective(s) of this one-year proof-of-concept SERDP SEED proposal was to: a). demonstrate environmentally-benign coating processes using conductive polymers (CP) as an alternative to hexavalent chromium (Cr(VI)) containing passivates; b). provide passivation and acceptable shell-to-shell contact resistance that will meet the requirements detailed in MIL-DTL-38999L, Class Z for CP coatings and c). show compatibility with, strong adhesion to, and corrosion-inhibition of the existing Low Hydrogen Embrittlement (LHE) alkaline Zn-Ni coatings.

Several objectives for these 2-layer CP coatings have shown the following promising results:

- 2- layer CP coating samples were tested for adhesion which showed excellent dry and wet tape adhesion,
- Excellent PATTI adhesion,
- Improved corrosion resistance properties via electrochemical impedance spectroscopy (EIS), a NSS exposure for the 2-layer CP coating,
- No hydrogen embrittlement after deposition of the 2-layer CP coating,
- The film morphology of the coatings was examined by scanning electron microscopy (SEM) and energy dispersive X-ray spectroscopy (EDS) revealed uniformly dense and defect-free coating,
- Did not meet the mil spec requirements for contact resistance before and after NSS, and
- This overall improvement in performance achieved from the 2-layer CP coating samples brings these coating materials to a promising performance level that would justify further and more detailed investigation.

9.0 Background

The use of zinc for anodic protection of ferrous substrates via a sacrificial mechanism has been well documented and commercialized by both private industry and the military.[1] Zinc plating has seen widespread use over the past several decades due to its effective and significant corrosion protection in aggressive environments and its economical application in commercial and military systems.[2,3] Zinc plating has been investigated as a replacement for current Cd plating of steel and steel alloys where severe corrosive environments and/or long lifetimes are not an issue. The main drawback to zinc as a replacement for Cd has been its relatively high corrosion rate. Therefore, Zn requires a thicker coating to provide a similar protection duration.[4,5] Additional drawbacks to using zinc metal are that zinc corrosion generates voluminous corrosion products that can cause seizure of close-fitting parts such as fasteners, and the hydrogen generated during the rapid corrosion of zinc metal contributes to hydrogen embrittlement (HE) of steel alloys.

Recent developments in electrodeposition and electroless deposition of zinc have focused on creating alloys that contain zinc with other elements such as manganese (Mn), iron (Fe), cobalt (Co), tin (Sn) and nickel (Ni).[6-8] These zinc alloys continue to provide sacrificial anodic protection, but with a lower corrosion rates. The lower corrosion rates allow thinner Zn-alloy films to provide formidable corrosion protection of the underlying metal substrate. The most promising of these alloys are the Zn-Ni alloys, which are reported to provide outstanding corrosion performance, and produce complex corrosion products that act as a barrier to diffusion of corrosive species. In addition, the finely cracked structure of Zn-Ni coatings disperse the anodic reactions throughout the coating, which mitigates localized corrosion.[9,10] One drawback to Zn-Ni alloys is that the electrodeposition baths are generally acidic and introduce hydrogen gas to the steel surface, which can result in HE.

Two alternate approaches to reducing hydrogen embrittlement are employ ternary or quaternary alloys,[3,11,12] or changing the bath/deposition conditions (concentration of additives, pH, temperature, current, pulsed or DC-current and flow conditions).[13,14] Zn-Ni alloys are still currently one of the most promising alternatives to Cd plating. Two environmental hazards (cyanide and Cd) are eliminated by using Zn-Ni plating baths. Cd and cyanide are highly regulated, and toxic.[15-17] The recent development of low hydrogen embrittlement (LHE) alkaline Zn-Ni plating baths, a viable, "environmentally-green" alternative to Cd plating is available. However, there remains a critical need for non-Cr(VI) passivates for commercialized Zn-Ni coatings. Commercial non-Cr(VI) passivates do not meet the requirements for contact resistance and are generally thicker, thus, requiring the toxic, carcinogenic, and highly regulated Cr(VI) passivate coating.[18-22]

This SERDP SEED has attempted to address several of these limitations by developing innovative passivates based on conductive polymers (CPs) that can be applied as films without releasing VOCs or HAPs and provide corrosion-inhibition, without affecting lubricity (wear resistance), or electromagnetic interference (EMI) shielding efficiencies (SE) of the underlying Zn-Ni coating.

CPs have been investigated at the laboratory scale and commercialized as viable corrosion-inhibiting coatings.[23] Polyaniline (PANI) has shown corrosion-inhibition via a passivation mechanism on steel substrates. PANI dispersions and PANI-containing lacquers were used to coat steel samples to provide primer layers of between 0.3-20 microns. The major accomplishments using these PANI dispersive layers was the ability of the corrosion potential to shift in the direction of the "noble region" as termed by Wessling.[24] PANI (CORRPASSIV^{TM}) containing primer paints have been commercialized, and this product has found widespread use in numerous countries throughout Europe and Asia in such diverse and corrosive environments as waste water treatment plants, construction materials (bridges), and commercial steel structures. Additionally, CPs have been investigated at the laboratory scale and field tested as a CCC replacement by researchers at the NAWCWD using poly(2,5-bis(N-methyl-N-hexylamino)phenylene vinylene) (BAM-PPV). This CP was field tested by the AF as a CCC coating replacement on the rear cargo hatch door of the C-5 Galaxy. BAM-PPV survived a one-year field test without any evidence of delamination or corrosion when compared to a fully Cr(VI) military coating.[25,26] The Army field tested BAM-PPV pretreatment in a non-Cr(VI) military coating system for a one-year field test on non-critical aluminum hardware (Bradley vehicle headlight cover) and found no evidence of corrosion or delamination.

CPs have unique properties that make them attractive alternatives to Cr(VI) coatings, namely their synthetic tailorability, environmental stability, redox activity, non-toxic nature, ease of doping, and high conductivities that are in the semiconductor range (10^{-2} to 10^{2} S/cm).[27] Additionally, CPs and chromium species undergo oxidation at similar potentials, which means that corrosive species that normally react with the chromium coatings will also react with the conducting polymers.[28]

Therefore, our efforts have focused on developing novel CPs that can be deposited onto Zn-Ni coated high strength steel coupons that can meet the requirements spelled out in the objectives section of this report.

10.0 Materials and Methods

10.1 NAWCWD Test Methods

10.1 Reagents and Spectroscopic Analysis

The following reagents were obtained from Aldrich Chemical and used without further purification: 3-aminophenol, *tert*-butoxycarbonyl, 1,6-diiodohexane, trimethylamine (TEA), dimethylformamide (DMF), 3,4-dimethoxythiophene, dimethylamine hydrochloride, triphenylphosphine, 3-aminophenol, di-*tert*-butyldicarbonate, (BOC anhydride), 3-chloro-1,2-propanediol, p-toluenesulfonic acid, thiophene-2-carbaldehyde, succinic acid, 1-methyl-1H-pyrrole, 3-(dimethylamino)acrylaldehyde, triethyphosphite, toluene, heptane, ferric chloride ($FeCl_3$) and tetrahydrofuran (THF). Nuclear Magnetic Resonance Spectroscopy (NMR) analysis were carried out on an Avance III Bruker 500MHz NMR spectrometer and Gas Chromatography/Mass Spectrometry (GC/MS) analysis were done using a Gas chromatography (GC) which was carried out on an Agilent 6890N GC using a Restek Rxi-4ms 30 m x 0.25 mm i.d. capillary column with a 0.25 μm coating of Crossbond 5% diphenyl/95% dimethyl polysiloxane. The GC was programmed from 40 to 300 °C at 20 °C/min. The GC detector was an Agilent 5973N mass selective detector (MSD).

Chemical polymerization of the diethyl ((2,3-dihydrothieno[3,4-*b*][1,4]dioxin-2-yl)methyl)phosphonate monomer was carried out using ferric chloride as initiator (1.5 equivalents) and the crude polymer was soxhlet extracted with DI water for 6 days to remove residual initiator from the polymer. The crude polymer was measured for iron (Fe) concentration via the following procedure: a portion of the polymer (~100 milligrams) is accurately weighed into a 50 milliliter polypropylene digestion vial. Approximately 15 mL of concentrated nitric acid (trace metal grade) is added to the vial. The vial is covered with a polypropylene watch glass and allowed to reflux at 90^{o}C for 2 hours. The solution is then cooled and brought to a final volume of 50 milliliters using 18 Megaohm deionized water. Any undigested polymeric solid present is filtered out of solution before analysis. Fe analysis was performed on a Thermo Fisher Scientific iCAP 6300 Inductively Coupled Plasma - Atomic Emission Spectrometer (ICP-AES). A CETAC autosampler coupled to a peristaltic pump, nebulizer, spray chamber, and argon plasma in a radial torch configuration. Detection of emission wavelengths between 166 and 847 nm is made possible by a charge injection device (CID). Data collection and analysis is performed using the Windows-based Thermo Scientific iTEVA software. The system is calibrated up to 10 ppm using certified calibration standards. The calibration curve is verified using a 1 ppm check standard prepared from a second source. Three replicate emission intensities are measured by the spectrometer, averaged, and converted to solution concentrations using the established calibration curve. Appropriate dilutions are made to any solutions containing iron concentrations above 10 ppm. Solution concentrations are back calculated to a weight percent (wt %) in the original solid sample. A reporting limit of 100 ppb (parts per billion) is used for the analysis.

10.1.2 Attempted Synthesis of the (6-(3-aminophenoxy)hexyl)phosphonic acid:

Described below is the attempted synthesis of the phosphonic acid derivative of the aniline monomer. The method which was used was described in the literature and was modified.[29] This modification of the literature procedure was attempted in order to obtain the target aniline phosphonic acid derivative which did not prove successful.

10.1.3 Synthesis of tert-butyl(3-hydroxylphenyl)carbamate:

10.0 grams of 3-aminophenol (0.092 moles) and 20.0 grams of BOC anhydride (0.092 moles) was dissolved in 40 ml DMF. A dropping funnel was charged with 10.6 grams TEA (0.105 moles) dissolved in 40 mL DMF. The addition of the TEA solution to the reaction flask was carried out slowly at 0ºC and kept at that temperature for 12 hours, solution then slowly allowed to warm to ambient temperature under a positive nitrogen blanket for 3 days. After 3 days, solution homogenous and was diluted with chloroform and DI water, and the pH of the aqueous layer was adjusted to 8 using 1.0N HCl. The aqueous solution was washed 3X with chloroform, and organic layer washed with saturated aqueous sodium bicarbonate solution. The organic solution was dried with $MgSO_4$, filtered, rotovapped and the oil dried under vacuum (0.05Torr, 25oC). The crude product was recrystallized from acetone/DI water, dried under vacuum (0.05Torr, 90ºC) to give an off-white powder in 6.9 grams in 36% yield (mp = 120-122ºC (uncorrected)). GC/MS confirmed product with purity of 97%. ^{1}H NMR (DMSO-d_6): 1.44 (s, 9H), 6.32 (dd, 1H), 6.95 (m, 1H), 7.00 (m, 2H), 9.14 (s, 1H), 9.21 (s, 1H). ^{13}C NMR (DMSO-d_6): 28.12, 78.79, 101.02, 103.35, 105.44, 109.17, 129.35, 140.54, 149.75, 152.67, 157.78, 158.05.

10.1.4 Attempted Synthesis of the *tert*-butyl(3-(6-iodohexyl)oxy)phenyl)carbamate:

Four attempts were performed reacting 1,6 diiodohexane with the BoC protected amino phenol. A typical procedure follows: 1.75 grams of 1,6 diiodohexane (5.2 mmol) was dissolved in 10 mL of DMF and 1.5 grams of potassium carbonate (11 mmol) was added. This mixture was stirred at 45ºC for 30 minutes. 1.0 grams (5.1 mmol) of the BoC protected amino phenol was dissolved in 10 mL of DMF and placed in a dropping funnel. The solution of the BoC protected amino phenol was added dropwise to the mixture over the course of 2 hours. The reaction mixture was stirred for 10 days. The mixture was poured into water, extracted twice with chloroform. The combined organic layers were extracted with water, then saturated sodium chloride, dried with MgSO4, filtered evaporated and dried under vacuum at 0.05 torr. In all cases, NMR analysis was inconclusive and GC/Mass Spectrometry had no indication of product.

This reaction proved unsuccessful and was abandoned in favor of the PEDOT derivative described below.

10.1.5 Synthesis of the 2-(chloromethyl)-2,3-dihydrothieno[3,4-*b*][1,4]dioxine:

This reaction was a repeat of an earlier literature preparation,[30] the results obtained matched the analysis of this known compound.

A mixture of 30.15 grams 3,4-dimethoxythiophene (0.209 moles), 21 mL 3-chloro-1,2-propanediol (0.251 moles, 1.2 eq.) and 1.0 gram p-toluene sulfonic acid in 500 mL toluene was refluxed overnight with a condenser set to 60°C. The mixture was cooled and washed with water then dried ($MgSO_4$). This was filtered through a short plug of silica gel then concentrated in vacuum to give 31.54 grams of a yellow liquid (79%). This was distilled under high vacuum (collected 86 to 93°C at 0.42 torr) to give 27.62 grams of a clear water white liquid (69%) (Figure 1) and confirmed by ^{1}H NMR ($CDCl_3$) 2.5 (s, 1H), 3.7 (m, 2H), 4.4 (t, 2H), 6.4 (dd, 2H) and GC/MS.

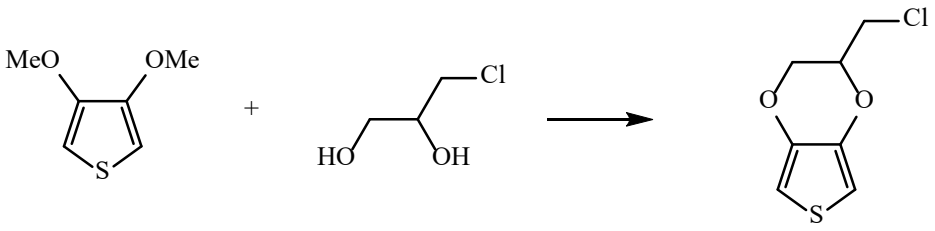

Figure 1. Synthesis of the 2-(chloromethyl)-2,3-dihydrothieno[3,4-*b*][1,4]dioxine

10.1.6 Synthesis of the diethyl ((2,3-dihydrothieno[3,4-*b*][1,4]dioxin-2-yl)methyl)phosphonate monomer: This represents a new phosphonate derivative of 3,4-ethylenedioxythiophene compound (EDOT).

A solution of 24.55 grams of the chloromethyl EDOT derivative (0.129 moles) in 200 mL triethyl phosphite (1.17 moles, 9eq) was refluxed for four days. Excess triethyl phosphite was distilled off under high vacuum to give 32.44 grams of a clear liquid. This was taken up in 100 mL toluene and 250 mL heptane. The solution was cooled to -20°C. The crystals were then filtered off and washed with hexanes to give 12.21 grams of small clear needles (32%) (Figure 2) and confirmed by GC/MS. ^{1}H NMR (Acetone-d_6): 6.44 (s, 2H), 4.45 (m, 1H), 4.35 (dd, 1H), 4.1 (m, 5H), 2.20 (dd, 2H), 1.31 (dt, 6H). ^{13}C NMR (Acetone-d_6): 141.41, 99.62, 99.38, 69.57, 67.80, 61.35, 26.59, 15.82. Calc for $C_{11}H_{17}O_5PS$: C 45.20%, H 5.86%, S 10.97%. Found C 45.28%, H 5.90%, S 10.83.

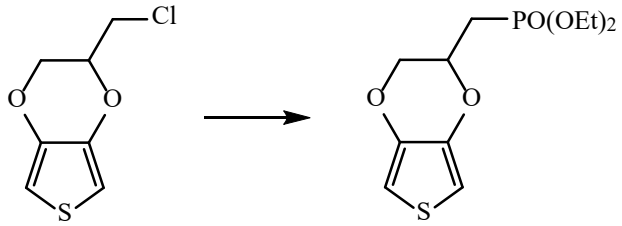

Figure 2. Synthesis of the diethyl ((2,3-dihydrothieno[3,4-*b*][1,4]dioxin-2-yl)methyl)phosphonate

10.1.7 Electrochemical Polymerization of diethyl ((2,3-dihydrothieno[3,4-*b*][1,4]dioxin-2-yl)methyl)phosphonate monomer:

A 128 mM solution of lithium triflate in propylene caboante was prepared. Approximately 250 mL of this solution containing 3g of diethyl ((2,3-dihydrothieno[3,4-*b*][1,4]dioxin-2-yl)methyl)phosphonate monmer was placed in a 400 mL beaker into which a Pt wire basket electrode was submerged. A 50 mL fritted thimble containing 9 g of $FeCl_3$ dissolved in the lithium triflate solution was used as a counter electrode compartment in the bulk electrolysis cell. A Pt basket was used as a counter electrode. A reference electrode (Ag^+/Ag , 12 mM $AgNO_3$ in acetonitrile) was placed near the Pt wire basket WE. The solutoin was set to electolyze at 1.3 V vs. reference for approximately 4 hours. During the electrolysis the solution turned from clear and colorless to a deep opaque blue color containing substantial amounts of deep blue solid material. Upon completion of the electrolysis the the solution and all solids from the WE compartment was placed in a large Erlenmeyer flask and 4 L of was DI water was added to precipitate any polymeric material. This solution was stirred for several hours, filtered, dried, placed in a Sohxlet extractor and extracted with acetone overnight. The acetone solution was deep blue in color and the solid remaining in the thimble was a deep blue/black color. Ostensibly, the acetone solution contains lower molecular weight polymer and the remaining solid is the higher molecular weight material. The high molecular weight material is insoluble in most common organic solvents, but it does show considerable solutility in m-cresol and furfuryl alcohol. The outer voltammogram shows the oxidation of the monomer occurs at approximately 1.1 V vs. ferrocene in acetonitrile (See Figure 3).

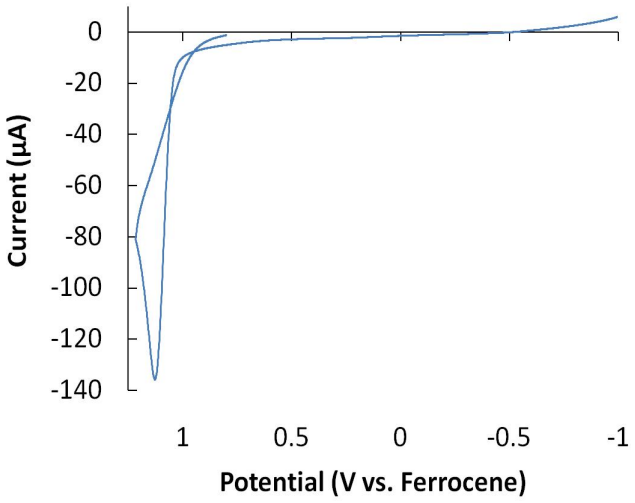

Figure 3. Voltammagram of the diethyl ((2,3-dihydrothieno[3,4-*b*][1,4]dioxin-2-yl)methyl)phosphonate monomer

The voltammogram shows three cycles of a poly(diethyl ((2,3-dihydrothieno[3,4-*b*][1,4]dioxin-2-yl)methyl)phosphonate) film on a gold electrode surface in an acetonitrile solution

with 100 mM tetrabutylammoium hexafluorophosphate as supporting electrolyte. The film is stable in the conductive (oxidized) state over a potential range of nearly 1.5V (Figure 4). Direct electrochemical deposition onto a ZnNi coated steel electrode from an acetonitrile solution was not successful. The ZnNi coating oxidizes before the monomer, leading to substrate corrosion. The rate of the corrosion increases with each cycle number (purple=cycle 1, red=cycle 50, blue= cycle 100) (Figure 5).

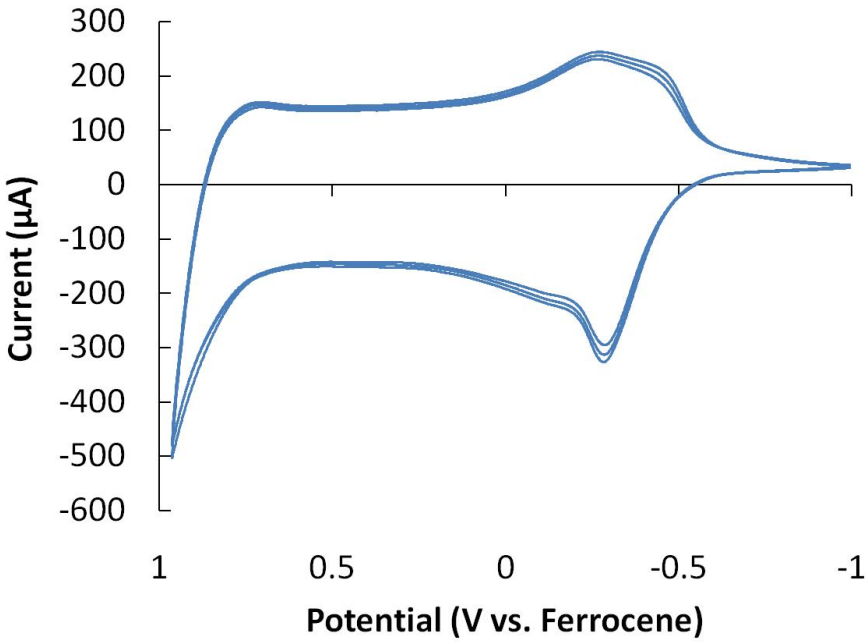

Figure 4. Cycling of the poly(diethyl ((2,3-dihydrothieno[3,4-*b*][1,4]dioxin-2-yl)methyl)phosphonate) film

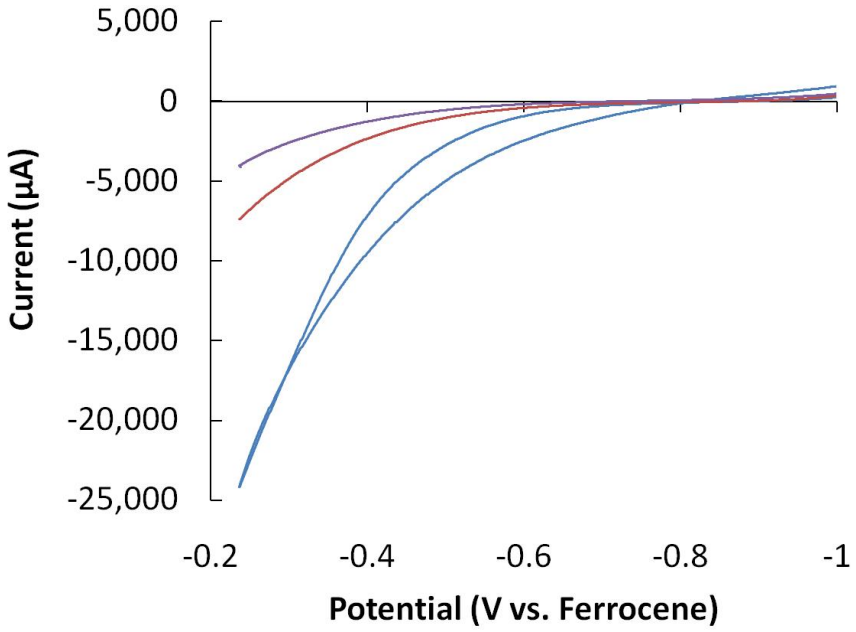

Figure 5. Direct electrochemical deposition of the diethyl ((2,3-dihydrothieno[3,4-*b*][1,4]dioxin-2-yl)methyl)phosphonate monomer onto a ZnNi coated steel electrode

10.1.8 Chemical Polymerization of the diethyl ((2,3-dihydrothieno[3,4-*b*][1,4]dioxin-2-yl)methyl)phosphonate monomer:

A 50 mL round bottom flask was charged with 20 mL anhydrous THF, 2.0 grams monomer (0.0068 moles), and $FeCl_3$ (1.5 equivalents, 1.7 grams, 0.010 moles). The contents of the round bottom flask were stirred for 6 hours under a positive nitrogen blanket in an oil bath maintained at 60°C. After 6 hours, solution heterogeneous, blue colored and the contents poured into 250mL DI water, stirred, filtered and the solid blue residue dried overnight in a vacuum desiccator (0.05 Torr, 25°C). The crude polymer was extracted with DI Water in a soxhlet extraction thimble for 96 hours. The polymer was dried under vacuum (0.05Torr, 25°C) overnight to give a blue-black powder in 1.2 grams (96% yield). The %Fe content after extraction was 1.7% (42.4 ppm), 98.3% of the residual $FeCl_3$ initiator was removed by this process. The polymer had limited solubility in a variety of solvents and the NAWCWD researchers were unable to obtain high quality films for further analysis.

10.1.9 Synthesis of Bis-substituted heterocyclic Butadienes:

Novel bis-substituted heretocyclic butadienes were examined as active self-healing CP coatings for this SERDP SEED. The synthesis and characterization of these compounds were under the Office of Naval Research, Program Manager, Dr. Airan Perez, Code 333. The following figures (Figures 6-11) document the synthesis of these materials and polymerization. The synthesis of the ((1-methyl-1H-pyrrol-2yl)methyl)triphenylphosphonium iodide, (E)-3-(1-methyl-1H-pyrrol-2-yl)acrylaldehyde and (1E, 3E)-1,4-di(thiophen-2-yl)buta-1,3-diene have been

reported in the literature.[31-33] However, the (1E, 3E)-1,4-bis(1-methyl-1H-pyrrol-2-yl)buta-1,3-diene has never been reported and represents a new monomer with interesting electrochemical and chemical polymerization properties.

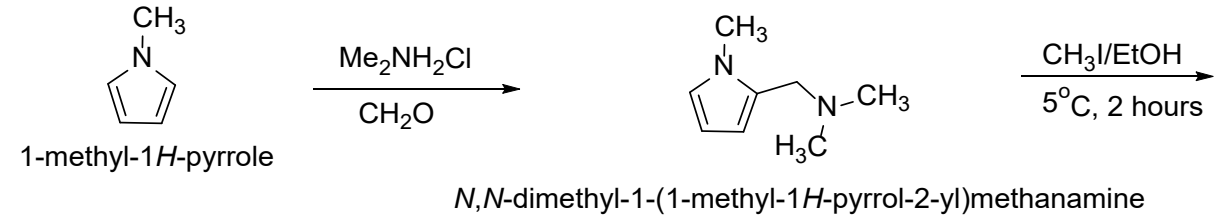

Figure 6. Synthesis of the N, N-dimethyl-1(1-methytl-1H-pyrrol-2-yl)methamine

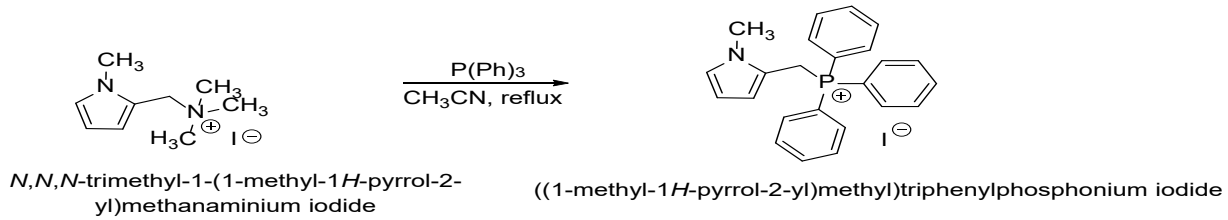

Figure 7. Synthesis of the ((1-methyl-1H-pyrrol-2yl)methyl)triphenylphosphonium iodide

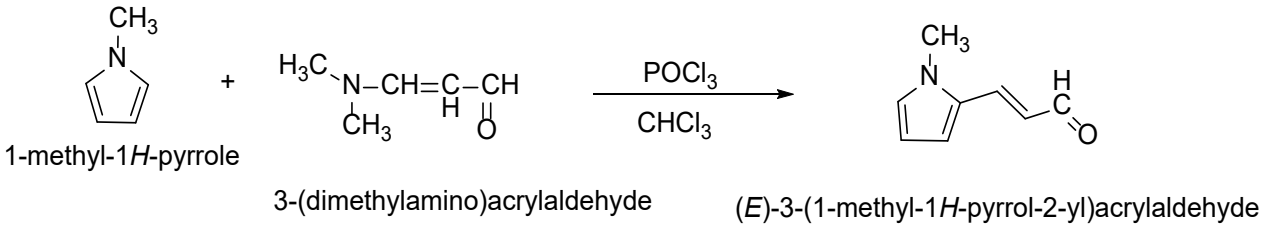

Figure 8. Synthesis of the (E)-3-(1-methyl-1H-pyrrol-2-yl)acrylaldehyde

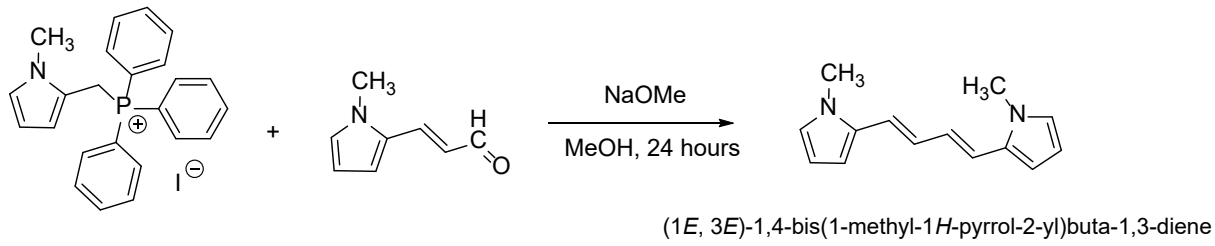

Figure 9. Synthesis of the (1E, 3E)-1,4-bis(1-methyl-1H-pyrrol-2-yl)buta-1,3-diene

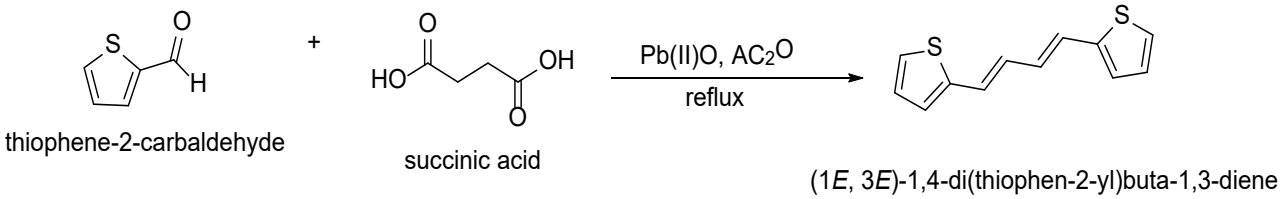

Figure 10. Synthesis of the (1E, 3E)-1,4-di(thiophen-2-yl)buta-1,3-diene

10.1.10 Electrochemical and Chemical Polymerization of the (1E, 3E)-1,4-di(thiophen-2-yl)buta-1,3-diene and (1E, 3E)-1,4-bis(1-methyl-1H-pyrrol-2-yl)buta-1,3-diene monomers:

Both the (1E, 3E)-1,4-di(thiophen-2-yl)buta-1,3-diene and (1E, 3E)-1,4-bis(1-methyl-1H-pyrrol-2-yl)buta-1,3-diene both undergo chemical polymerization (Figure 11), and electrochemical polymerization (Figure 11). The oxidation potential of the (1E, 3E)-1,4-bis(1-methyl-1H-pyrrol-2-yl)buta-1,3-diene is very low, thereby offering a potential self-healing mechanism when incorporated into polymer host. Unfortunately the solubility of the poly[1,4-di(thiophen-2-yl)buta-1,3-diene] was very limited, thereby precluding the fabrication of acceptable films for incorporating the active monomer, (1E, 3E)-1,4-bis(1-methyl-1H-pyrrol-2-yl)buta-1,3-diene into the host CP.

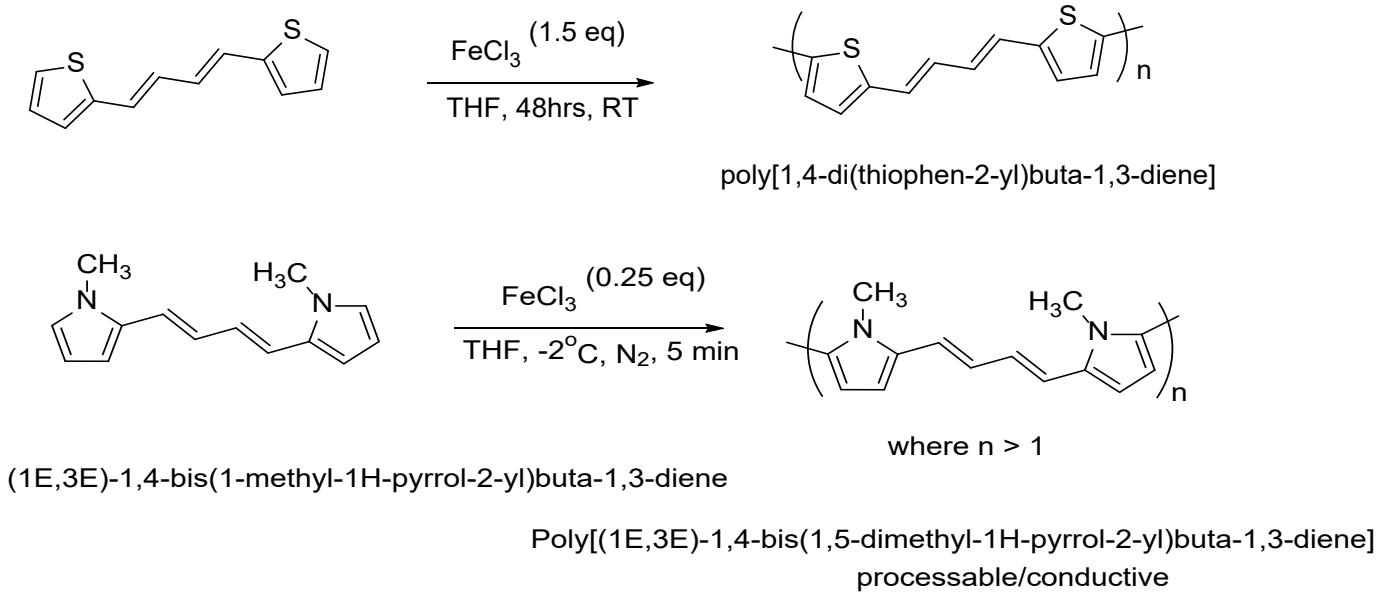

Figure 11. Chemical Polymerization of Both Bis-heterocyclic butadiene Monomers

The electrochemical polymerization of the (1E, 3E)-1,4-bis(1-methyl-1H-pyrrol-2-yl)buta-1,3-diene monomer is shown in Figure 12 below. All voltammetry was performed using 240 mM tetrabutylammonium hexafluorophosphate ($TBAPF_6$) in acetonitrile as a supporting electrolyte solution. The same non-aqueous reference was used for all measurements (silver wire in 100 mM $AgNO_3$ and 100 mM $TBAPF_6$ in acetonitrile solution separated by Vycor frit). All scan rates were

100 mV/s. Monomer concentration during polymerization was ~4 mM. The monomer oxidizes at 0 V, which is very low for most pyrrole monomers. The current increases with cycle number, indicating the formation of an electroactive film.

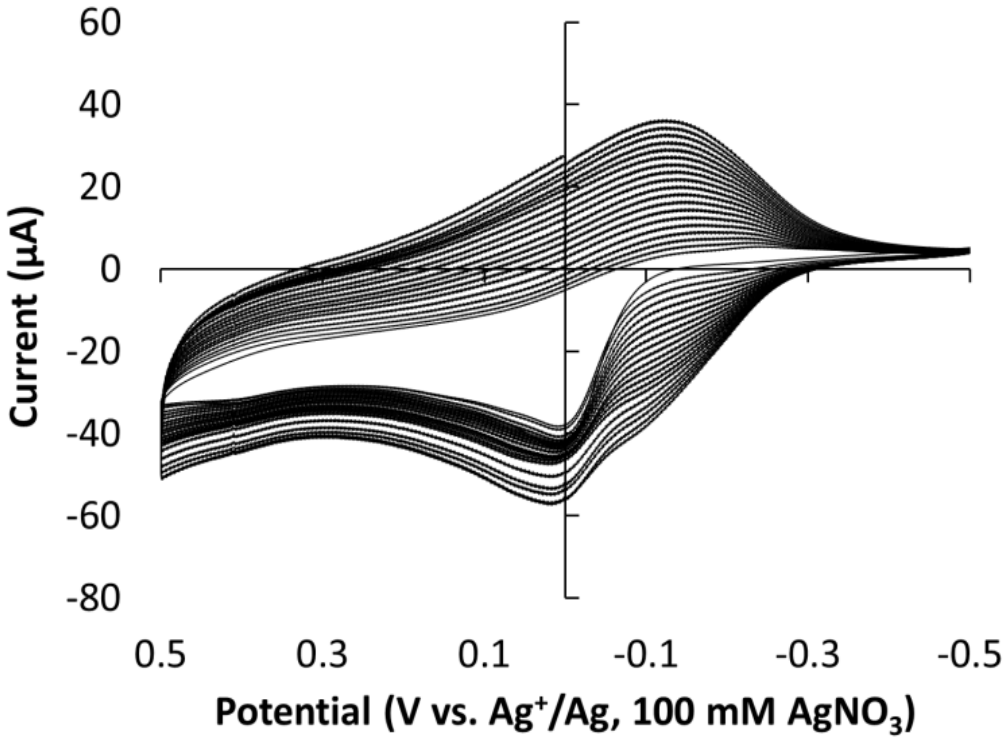

Figure 12. Electropolymerization of the (1E, 3E)-1,4-bis(1-methyl-1H-pyrrol-2-yl)buta-1,3-diene monomer

The polymerization of the (1E, 3E)-1,4-di(thiophen-2-yl)buta-1,3-diene monomer is shown in Figure 13. In this case the monomer oxidizes at 0.6 V, and again the current increases with cycle number indicating the formation of an electroactive film.

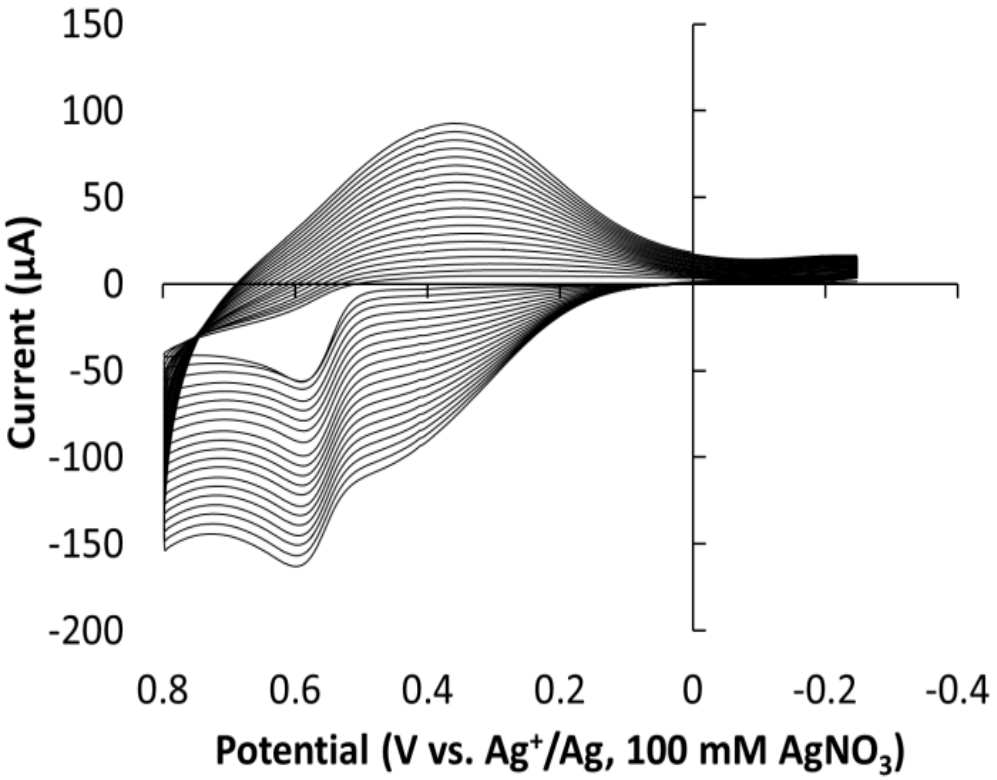

Figure 13. Electropolymerization of the (1E, 3E)-1,4-di(thiophen-2-yl)buta-1,3-diene monomer

10.1.11 NAWCWD - Films for corrosion protection analysis were prepared as follows for NAWCWD and WPAFB/UDRI :

A 1.1% solution of high molecular weight poly(diethyl ((2,3-dihydrothieno[3,4-*b*][1,4]dioxin-2-yl)methyl)phosphonate) in furfuryl alcohol was stirred at ambient temperature for approximately 3 weeks. Intially, this solution is deep blue in color. Over time, the color changes to brown and the solution turns into a paste. To prepare a coating solution 3.16 g of this brown paste was dissolved in 30 g of acetone and stirred until dissolved. The solution was deep brown, but contained no visible particulates. Approxmately 2 mL of this solution was dropped onto ZnNi coated steel substrates that were approximately 1" x 4". The solution was spread over the entire surface using the end of a pipet. The substrates were placed in an oven at 100ºC for 24 hours, removed and cooled to ambient temperature, the films were dry to the touch.

10.1.12 Electrochemical Impedance Spectroscopy (EIS) Measurements on 2-layer poly(diethyl ((2,3-dihydrothieno[3,4-*b*][1,4]dioxin-2-yl)methyl)phosphonate) films:

EIS measurements on the single coating (1L) indicated corrosion (Figures 14 and 15), so a second layer was added followin the same procedure. Resistivity measuremens were performed by sandwiching the substrate between two 0.75" copper diske electrodes. EIS measurements mainly acted as a screening tool. The data were collected at the open circuit potential with an AC

amplitude of 10 mV. Analysis was performed qualitativly, focused mainly on the shape of the lower frequency region of the Nyquist plot and on the differences between spectra over time for indiviudal samples.

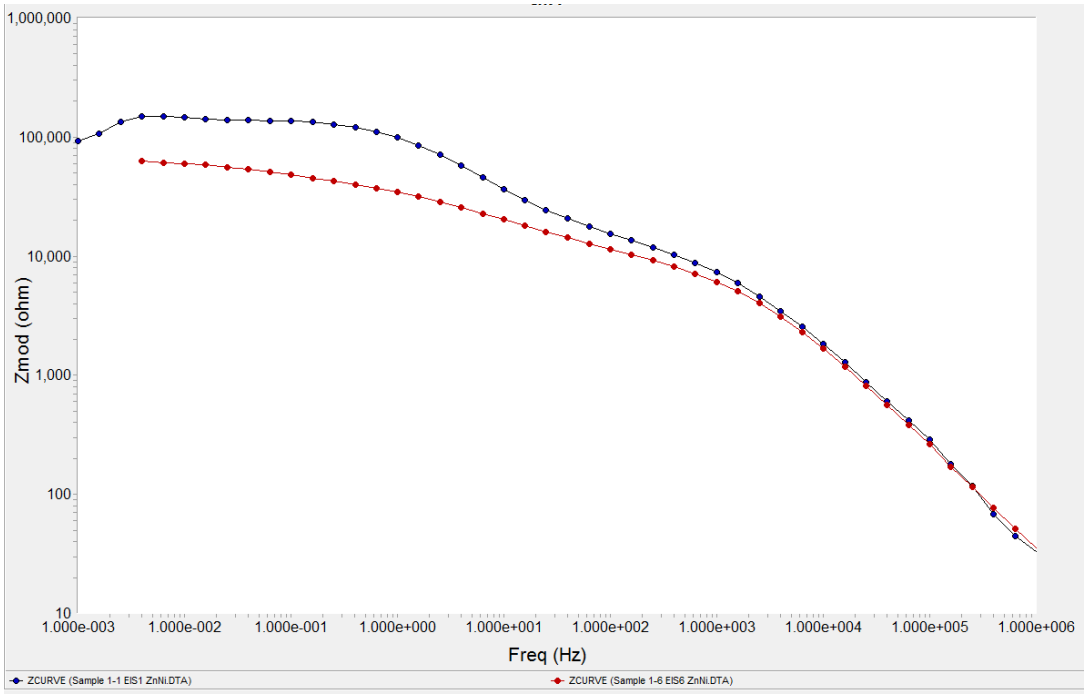

Figure 14. Bode Magnitude plot for substrates with 1 layer of polymer coating

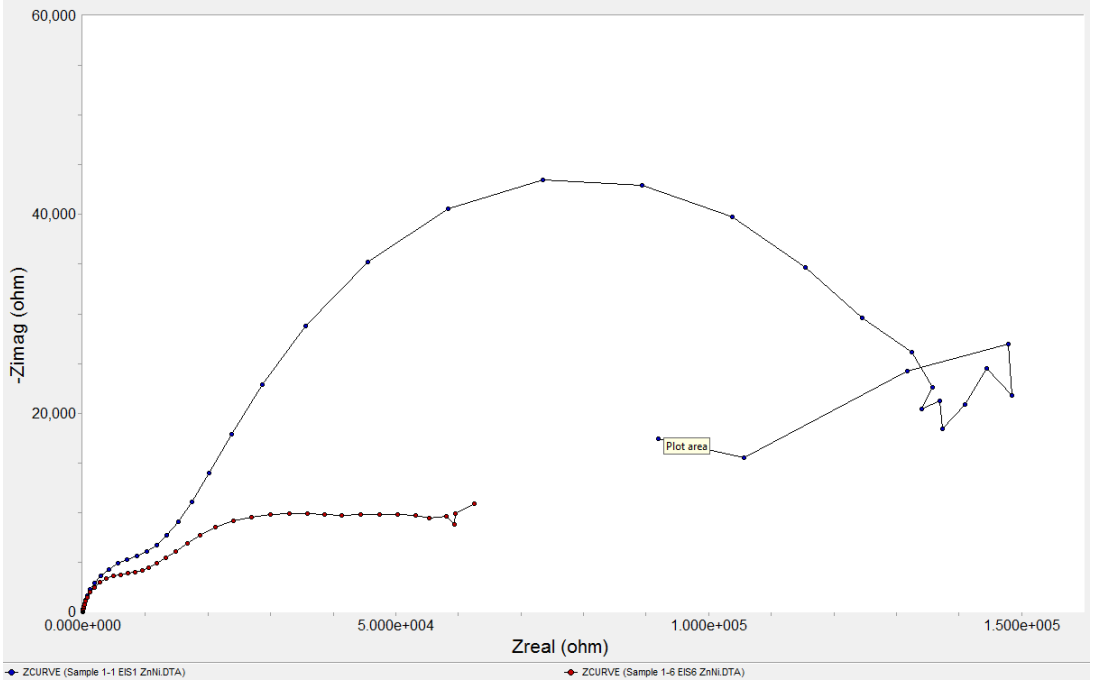

Figure 15. Nyquist plot for substrates with 1 layer of polymer coating

Figure 14 shows a represenative example of what we observed for substrates with only one coating of polymer. The magnitude of the impedance for samples at low frequency was relatively high, which we took as a positive sign. However, over the course of 24 hours the magnitude declined. Further evidence that the underlying coating was corroding is shown in Figure 15. The Nyquist plot for the initial spectrum is larger of the two arcs shown in the figure. At the low frequency (right most) region, the data become noisy and the points collected at the lowest frequencies actually cycle back under the arc; a classic sign of corrosion. The spectra collected after 24 hours shows that the low frequency resistance is significantly lower in magnitude than the initial spectra. We hypothesized that these issues were the result of a non-uniform coating that had defects leaving the underlying metal substrate exposed. To mediate these effects, we added a second layer of polymer coating.

The EIS spectra for the substrates with 2 layers of poly(diethyl ((2,3-dihydrothieno[3,4-*b*][1,4]dioxin-2-yl)methyl)phosphonate) are similar. They both create the same arc structure, and the low frequency resistance decreases with time (Figure 16). The low frequency data in the Nyquist plot (Figure 17) does not circle back under the arc in the case of the subtrates with 2 layers of polymer though. We took this as a positive sign for inhibiting corrosion and further studies were done on 2-layer coatings.

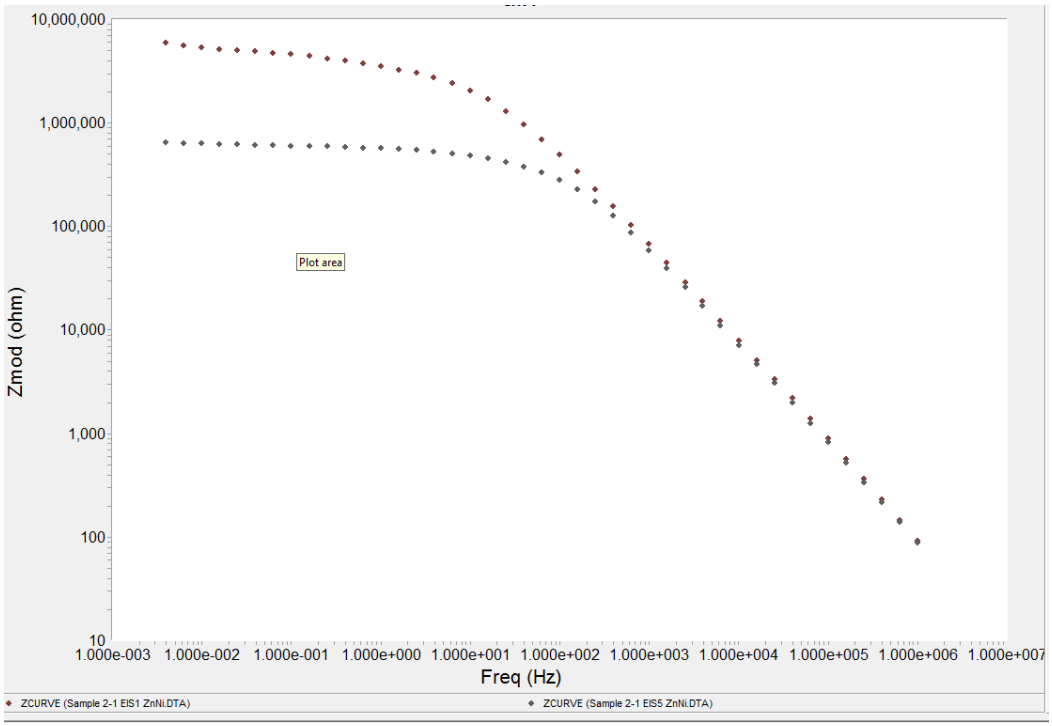

Figure 16. Bode Magnitude plot for substrates with 2 layers of polymer coating

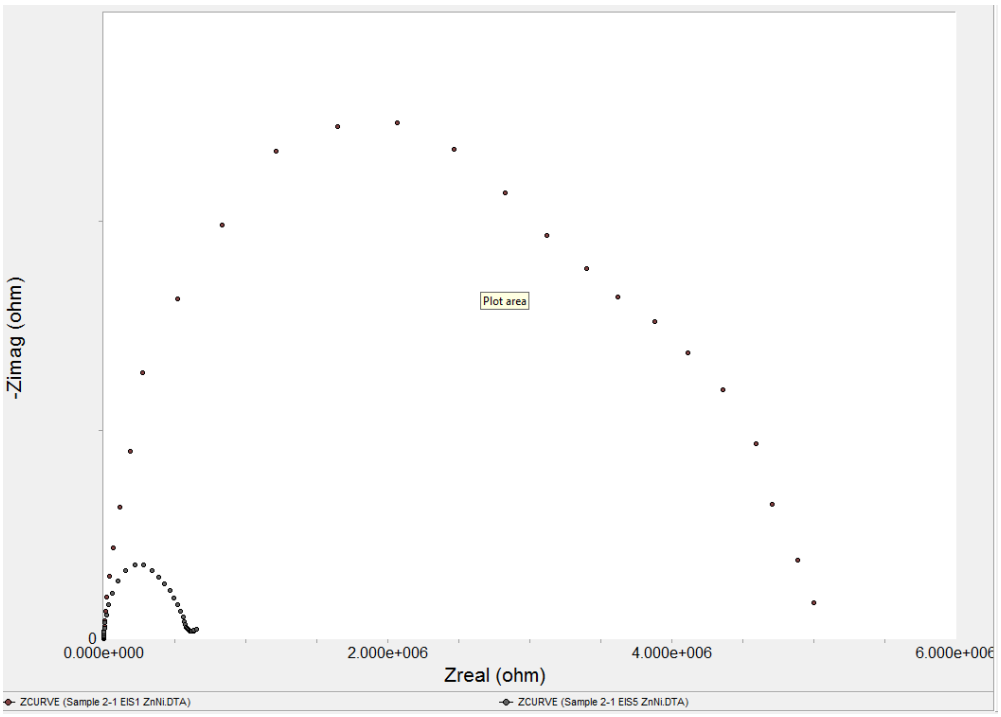

Figure 17. Nyquist plot for substrates with 2 layers of polymer coating

10.2 NAWCWD Testing Procedures

10.2.1 Coating Thickness Measurements at NAWCWD

Three measurements were made at five locations, see Figure 18, on each panel. Measurements were conducted using a Defelsko Positector 6000, which measures coating thickness by eddy current and the results are summarized in Table 1.

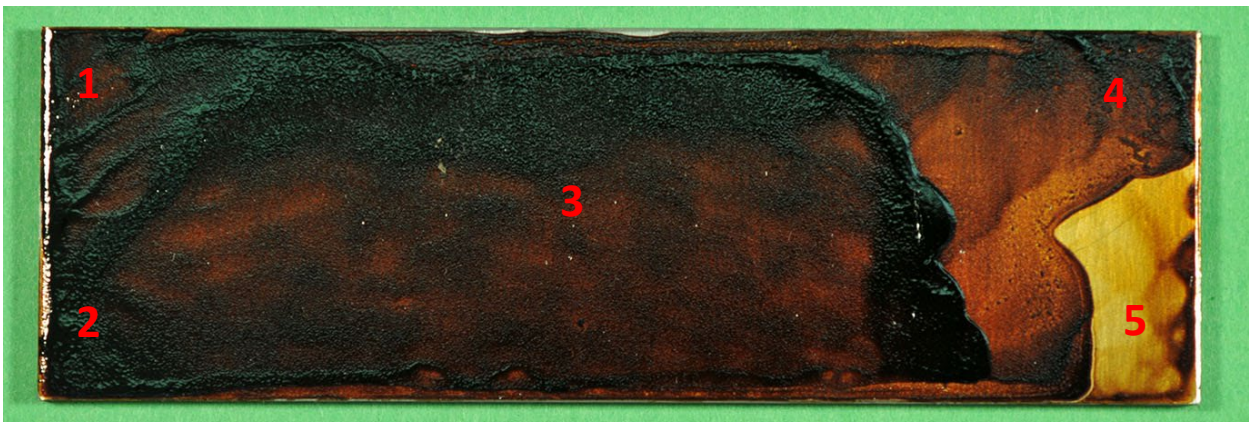

Figure 18. Locations of coating thickness measurements for 2L coating

Table 1. Coating Thickness of All CP Coated Zn-Ni Panels (mils)

Test	Loc 1	Loc 2	Loc 3	Loc 4	Loc 5	Average
Patti A	3.4	3.1	1.0	1.8	1.6	2.2
Patti B	0.9	0.9	0.9	1.2	1.2	1.0
Patti C	2.4	1.0	1.1	1.7	1.4	1.5
Wet Adhesion A	0.8	1.4	1.1	1.5	1.2	1.2
Wet Adhesion B	1.0	1.6	1.4	1.3	1.5	1.4
Wet Adhesion C	1.5	1.6	1.0	2.4	1.0	1.5
Dry Adhesion A	1.4	1.0	1.1	1.1	1.2	1.2
Dry Adhesion B	1.8	1.5	1.2	1.0	1.0	1.3
Dry Adhesion C	4.1	1.7	1.2	1.7	1.8	2.1
NSS A	1.0	1.2	1.2	1.3	0.7	1.1
NSS B	1.2	1.4	2.1	1.2	1.2	1.4
NSS C	1.5	1.5	1.2	1.0	1.0	1.2
NSS D	1.2	1.4	1.3	1.2	2.1	1.4
NSS E	1.8	1.1	1.2	1.3	1.2	1.3
Misc A	1.1	1.2	1.2	1.9	0.8	1.2
Misc B	1.6	2.1	1.5	1.8	1.5	1.7
Misc C	1.7	1.4	1.2	1.5	1.9	1.5
Misc D	2.0	2.2	1.4	2.0	1.4	1.8
Misc E	1.3	1.3	1.2	1.8	1.2	1.4
Misc F	1.0	1.6	0.9	1.3	1.4	1.2

10.2.2 Dry Tape Adhesion Testing at the NAWCWD:

Three tests were made on each panel. Because the coating thicknesses were generally less than 2 microns, the spacing between scribes was 1mm. This is in accordance with ASTM D3359. Eleven scribes were made in both perpendicular directions. After scribing with the pattern, 3M No 250 tape was applied and pressed to the panel using a rubber eraser.

10.2.3 Wet Tape Adhesion Testing at the NAWCWD:

Testing was performed in accordance with FED-STD-141 Method 6301.3. The panels were soaked in distilled water for 24 hours, after which they were removed, wiped dry, and scribed. 3M No 250 tape was applied, a 4-1/2 lb. rubber roller applied pressure, and the tape was removed.

10.2.4 Pull-off adhesion testing - Tensile Adhesion (Pneumatic Adhesion Tensile Testing Instrument (PATTI Test)) (PATTI) at the NAWCWD:

Pull-off adhesion testing was performed in accordance with ASTM D4541 test method E. All testing was performed in a laboratory, at standard pressure, temperature, and humidity. The test used a self-aligning adhesion tester type V, the PosiTest Pull-Off Adhesion Tester. The loading fixtures used were PosiTest AT Dollies, 20mm diameter. The bearing ring is 1.15 inches in diameter. All panels were rinsed with isopropyl alcohol and dried before adhering loading fixtures. Loading fixtures were adhered to the panel surfaces using the PosiTest Adhesive Kit. Two fixtures were applied per panel. No scoring around the dollies was employed in the course of these tests. All tests were run at roughly 50 psi/s. After the first test (Patti C), a shockwave went through the panel and knocked the second test dolly off. Following this, the remaining panels were cut in half using a band saw. The remaining tests occurred without issue.

10.2.5 Neutral Salt Sprat Testing (ASTM B117) at the NAWCWD:

Samples were tested in accordance with ASTM B117 in an Ascott S120XP salt fog chamber. The water used was deionized using an in-house filtration system. The salt was Morton Culinox Food Grade Salt. New neutral 5% salt solution was made daily on weekdays, and on some Saturdays. The deionized water conductivity was in the range of 1.0 – 4.6 microohms. Within the fog chamber, the temperature readings were consistently 35.0°C over the course of the test. During the test fallout was collected in 80 cm^2 funnels, ranging from 1.42 – 2.95 mL/hour of fallout per device. On 8 occasions (of 15) the fallout exceeded the 2.0 mL/hr. limit set by the standard. Fallout pH was measured daily; it varied from 6.81 to 7.24. It exceeded the limit of 7.2 on one occasion. The salt concentration of the fallout was measured daily, values ranged from 4.8% to 5.2%. The test chamber contained the five panels with candidate coating, as well as several painted steel panels with for another customer. None of the samples for this report were scribed. Specimens were protected on the edges using paraffin wax to limit corrosion. Specimens were not cleaned

and were minimally handled. All specimens sat vertically on a plastic rack, spaced 1 inch between specimens. Testing was paused every 100 hours, at which point the samples were removed and photographed. When the samples began to blister, photographs with intense side lighting were taken in order to better show the blisters. The chamber was also opened at 240 and 334 hours to service additional panels. The duration of the test chamber being opened was not over 2 hours.

10.3 WPAFB/UDRI Testing Procedures

The tests described in this report were performed according to UDRI Laboratory Procedures and Work Instructions as defined in the ISO/IEC 17025 Scope of Accreditation for the University of Dayton Research Institute Coatings, Corrosion & Erosion Laboratory. All testing was conducted in accordance to the test plan outlined in the SERDP/SEED WP-2525 research proposal.

10.3.1 Test Coated Samples at WPAFB/UDRI

The CP coating samples were provided by the NAWCWD for testing and evaluation in two consecutive batches, designated as 1L and 2L coatings. The coating materials were applied at the NAWCWD on the UDRI-prepared Zn-Ni electroplated steel substrates. The electroplating of steel panels was performed according to the following procedure.

10.3.2 Preparation of zinc-nickel plated panels at WPAFB/UDRI

Low-hydrogen embrittlement alkaline zinc-nickel (Zn/Ni LHE) plating was performed on 4130 steel substrate using the Dalistick mobile electroplating work-station unit. The 4130 steel panels were initially degreased with MEK by wiping them off with MEK-soaked cotton sample cloth. Spots of rust and the occasional sharp edges of the panels were sanded off with sand paper to prevent damage of the padding in the electroplating brush of the Dalistick instrument. Then the panels were activated using Dalistick and a Dalic Activator XF solution. After activation, the panels were electroplated using Dalic Zinidal Aero 11040 solution. Once electroplated, the panels were rinsed with DI water, hand-scrubbed with abrasive maroon Scotch-Brite (3M) pads, rinsed again with water, wiped with paper towels and air-dried in ambient conditions.

The whole surface of the panel (4x6 inches) was electroplated with the average thickness of Zn-Ni layer at 13 μm. The thickness of the electroplated coating was controlled by the pre-programmed delivery of the electric current through the Dalistick work-station. After electroplating, the thickness was confirmed with the PosiTector thickness gage. The analysis of the electroplated material was performed by the Thermo Scientific portable XRF analyzer XL2. To obtain statistically proven data, 6 (out of 24) evenly selected panels were analyzed by XRF with 3 measurements per plate in 3 different spots over the panel surface. On average, it was found

10.6±0.3% of nickel and 71.6±3.9% of zinc present within electroplated coating. The portable XRF was used as a screening method for rapid analysis of the Ni-Zn ratio to determine if WPAFB was getting consistent Zn-Ni alloy deposition throughout the entire surface of a sample and to assess sample-to-sample variability. The majority of other constituents to reach the total sum of 100% comes from the iron substrate. However, a summation of all the constituents was never a goal since it was expected to be affected by different factors such as uncertainty in surface chemistry of the steel substrate and the proprietary nature of the electroplating solution.

The coatings were applied via a drop casting method by placing a small amount of acetone-based polymer solution on a Zn-Ni-plated steel panel with the size of approximately 1×6 inches. The solution was spread and then allowed to evaporate to form a film. For the first batch of coating samples (1L coatings), the coated area was limited to a round spot located in the middle of a steel panel with the approximate size of 7-8 square centimeters. The 2L coating samples were prepared in a similar manner; however, these coatings cover the whole area of 1x6 inch steel panels, as the larger volumes of polymer solution were applied. Additionally, as the "2L" designation reflects, this group of coating samples was prepared by applying two layers of coating material with a quick drying time between layers, so the first layer was still tacky. Due to such two-layer application process, the 2L coatings were much thicker than 1L coatings samples.

10.3.3 Test Descriptions at WPAFB/UDRI

10.3.4 Dry Film Thickness Measurement at WPAFB/UDRI

The dry film thickness (DFT) of coatings on steel substrates was measured non-destructively by a PosiTector 6000 (DeFelsko, NY, USA) using a combination magnetic/eddy current probe. The meter was standardized according to manufacturer's instructions prior to each use. Multiple readings were taken. Data and calibration data were reported. Measurements were performed following UDRI Laboratory Procedure CLG-LP-003, Dry Film Thickness.

10.3.5 Crosshatch Adhesion Testing at WPAFB/UDRI

The test helps in evaluating adhesion between a coating and underlying substrate as well as the intercoat adhesion between all layers of the coating system. Crosshatch adhesion of each coating system was determined according to ASTM D3359, *Standard Test Methods for Measuring Adhesion by Tape Test; Method B* (Tables 2 and 3). This testing was performed following UDRI Laboratory Procedure CLG-LP-008, Tape Test Adhesion, Method B. For the test, a 0.5 x 0.5 inch crosshatch grid was cut through the coating and tape was firmly applied and pulled off at a 180º angle. The results were rated by a visual examination of the paint at the crosshatch-cut area according ASTM D3359 using the following rating scale, with ratings of 4B and 5B considered adequate:

- 5B – 0% of area removed
- 4B – less than 5% of area removed
- 3B – 5-15% of area removed
- 2B – 15-35% of area removed
- 1B – 35-65% of area removed
- 0B – greater than 65% of area removed

Table 2. ASTM D3359 Method B Crosshatch Adhesion Rating Scale

Adhesion Rating	Description
5A	No peeling or removal
4A	Trace peeling or removal along incisions or at their intersection
3A	Jagged removal along incisions up to 1/16 in. on either side
2A	Jagged removal along most of the incisions up to 1/8 in. on either side
1A	Removal from most of the area of the X under the tape
0A	Removal beyond the area of the X

Table 3. Rating Scale, Crosshatch Testing (Method B)

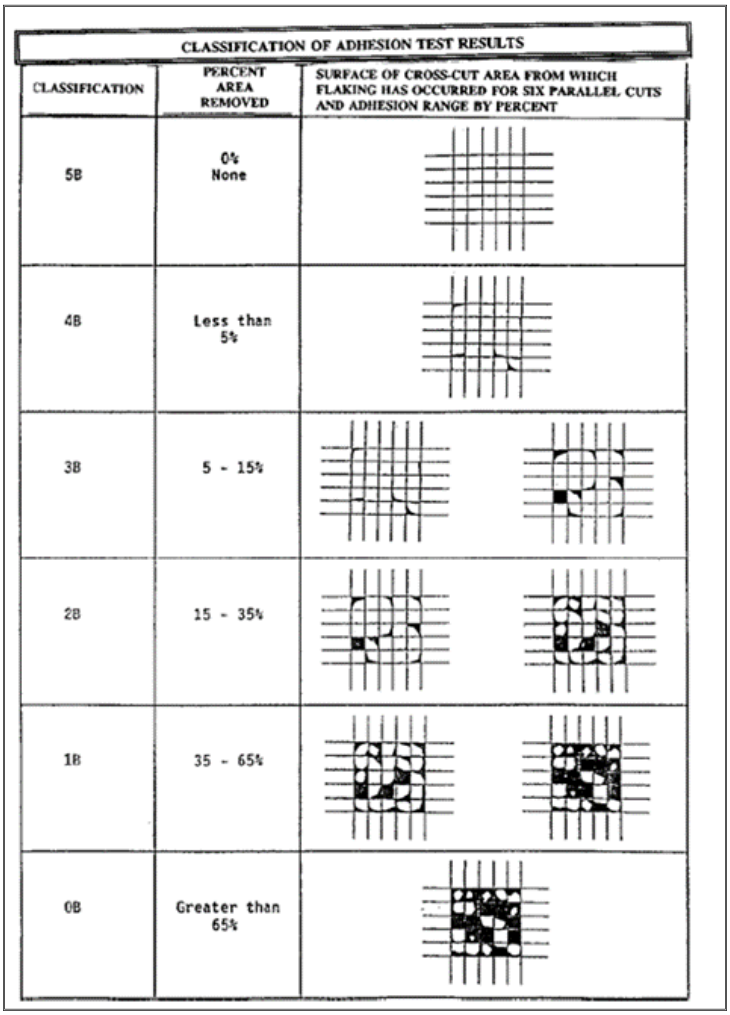

CLASSIFICATION OF ADHESION TEST RESULTS

CLASSIFICATION	PERCENT AREA REMOVED	SURFACE OF CROSS-CUT AREA FROM WHICH FLAKING HAS OCCURRED FOR SIX PARALLEL CUTS AND ADHESION RANGE BY PERCENT
5B	0% None	
4B	Less than 5%	
3B	5 - 15%	
2B	15 - 35%	
1B	35 - 65%	
0B	Greater than 65%	

Detailed description of the test procedure is provided below:

10.3.6 UDRI Laboratory Procedure CLG-LP- 003, Dry Film Thickness

The dry film thickness of coatings on ferrous and nonferrous metallic substrates is measured non-destructively by using a combination magnetic/eddy current probe. The meter is standardized according to manufacturer's instructions prior to each use. Multiple readings are taken. Data and calibration data are reported using ASTM D 7091, Standard Practice for Nondestructive Measurement of Dry Film Thickness of Nonconductive Coatings Applied to Ferrous Metals and Nonmagnetic, Nonconductive Coatings Applied to Nonferrous Metals and Applicable dry film thickness gauge owner's manual (e.g. DeFelsko DFT gauge PosiTector 6000).

10.3.7 Wet Tape Adhesion Test at WPAFB/UDRI

The wet tape adhesion test is intended to evaluate the adhesion performance for the coating systems immersed in deionized water for at least 24 hours. This testing is normally performed following UDRI Laboratory Procedure CLG-LP-033, Tape Test Adhesion, according to MIL- PRF-32239A, Section 4.6.13 Wet Tape Test. The procedure follows MIL-PRF-23377K, *Performance Specification, Primer Coatings: Epoxy, High-Solids,* and MIL-PRF-85285E, *Performance Specification: Coating, Polyurethane, Aircraft and Support Equipment*. The rating scale typically used for samples evaluation is shown in Table 4 and it is based on the rating scale described in ASTM D3359 Method A which requires the evaluation of an X-cut made through the coating**.** On provided samples however, the area of coating was relatively small due to limitations of the drop-casting method used for coating application. Therefore, due to space constrains, a modified procedure was used for a wet tape adhesion test. The modification involved the scribing of samples that was performed according to a cross-hatch adhesion method described in the Laboratory Procedure CLG-LP-033, Tape Test Adhesion, Method B. The crosshatch scribed pattern typically occupies only 0.5x0.5-inch space that was small enough to scribe all provided samples consistently. For both dry and wet tape adhesion tests, we used a cross-hatch pattern to make a cut through the coatings. Therefore, the correct rating scale should be for "method B" in all places for both groups of samples. Method A, which requires X-cut was never used, as we were limited by the dimensions of the small samples. The method A is included in this document for instructive purposes only.

Table 4. Rating Scale for ASTM D3359 Method A

Adhesion Rating	Description
5A	No peeling or removal
4A	Trace peeling or removal along incisions or at their intersection
3A	Jagged removal along incisions up to 1/16 in. on either side
2A	Jagged removal along most of the incisions up to 1/8 in. on either side
1A	Removal from most of the area of the X under the tape
0A	Removal beyond the area of the X

For wet tape adhesion testing, the uncoated surface of the steel coupons was masked off using electroplating tape in order to prevent corrosion of steel substrate. The panels were immersed in de-ionized water for 24 hours at room temperature. After immersion, the samples were dried and allowed to sit at ambient conditions for 3 minutes. The electroplating tape was removed to

prevent interference with scribing tool. A crosshatch pattern was scribed through coating down to the substrate. A strip of 1-inch-wide masking tape, such as 3M 250 or equivalent, was applied. The tape was pressed down using finger pressure, followed by rubbing with a pencil rubber eraser. The tape was removed in one abrupt motion perpendicular to the panel. The adhesion was rated by a visual examination of the paint at the crosshatch-scribed area using the rating scale in ASTM D 3359 Method B.

10.3.8 Tensile Adhesion (Pneumatic Adhesion Tensile Testing Instrument (PATTI Test)) at WPAFB/UDRI

The coated samples were tested in accordance to ASTM D 4541, Standard Test Method for Pull-Off Strength of Coatings Using Portable Adhesion Testers (PATTI). The testing was performed following UDRI Laboratory Procedure CLG-LP-046, Tensile Adhesion. The procedure follows ASTM D 4541 (test method D) using a type IV self-alignment tester, described in annex A3 of ASTM D 4541.

The PATTI adhesion testing uses an axial tensile pull test of a stud glued to a substrate using epoxy adhesive. During sample preparation, test area was lightly abraded with 800 grit sandpaper before the stud is adhered to the coating to achieve a stronger bond between the epoxy and the coating layer. Then, an adhesive mask was placed on the test area to limit the contact area of the epoxy adhesive to the area of the stud. The adhesive was allowed to cure in oven at 66°C for the duration of 24 h. Once the epoxy was cured, the stud was pulled using a self-aligning, pneumatic piston of the PATTI instrument until separation occurred between the stud and the substrate surface. This rupture pressure was recorded and then converted into tensile strength (psi) according to a table collected for the appropriate piston/stud pair. Detailed description of the test procedure is described below: *[UDRI Laboratory Procedure CCEG-LP-046, Tensile Adhesion (PATTI Test)]*.

The procedure follows ASTM D 4541, according to test method D, using a type IV self-alignment tester, described in annex A3 of ASTM D 4541. The test area is lightly abraded with 400-grit sandpaper and then wiped with IPA to remove dust, an adhesive mask is applied to isolate the test area, and then a pull stud is glued to the exposed surface. After the glue cures, the stud is pulled off and the pull-off pressure is recorded. The recorded gage pull-off pressure psig is converted to the pull-off tensile strength using the following instrumentation Quantum Series Operator's Manual under guidance from ASTM D 4541 – Standard Test Method for Pull-off Strength of Coatings Using Portable Adhesion Testers.

Conversion Chart: PSIG to PSI for F-8 Piston Formula: psi = [(ba)-c]/d

b = burst pressure from gauge (psig)

a = contact area of the gasket in the F-8 piston = 7.95 square inches

c = piston constant for F-8 = 0.51 lbs +/- 1.5%

d = contact area of the pull-stub = 0.196 square inches

Dixon Criteria (outlier evaluation and exclusion per ASTM E 178)

Outlier Equations

Qexp = $\left|(x2 - xq)/(xn-1 - xq)\right|$ for smallest value suspected

Qexp = $\left|(xq - xn-1)/(xq - x2)\right|$ for largest value suspected

Where

xq is the suspect value

xn is the largest value in the data set

x2 is the second smallest value in the data set

xn-1 is the second largest value in the data set

10.3.9 Neutral Salt Spray Test at WPAFB/UDRI

The neutral salt spray (B117) test was performed following UDRI Laboratory Procedure CCEG-LP-019, Salt Spray Corrosion. The test specimens of conductive polymer coatings were not scribed. The coated area of the steel substrate was masked off using the electroplating tape to prevent undesirable corrosion of the uncoated substrate. The coated panels were mounted at 15° angle from vertical and placed in a Q-Fog Cyclic Corrosion Test Chamber. The chamber exposure was performed in accordance with ASTM B 117 with the salt spray application using 5% sodium chloride (NaCl) solution with the adjusted pH in range of 6.5 to 7.2. Panels were visually evaluated at 100 h increments of exposure. Before the visual examinations, the exposed panels were thoroughly rinsed with tap/de-ionized water and then dried.

10.3.10 Hydrogen Embrittlement (HE) Susceptibility Testing Results at WPAFB/UDRI

The hydrogen embrittlement (HE) testing was performed by the AFRL/RXSA Materials Test and Evaluation Lab (MTE) on 12 provided specimens, 8 of the 12 specimens were coated with 2L conductive polymer coating, the remaining 4 specimens were uncoated to provide baseline untreated samples. Three Satec lever arm creep testing (stress rupture) mechanical test frames were used to perform HE testing. The test specimens were obtained from the manufacturer (Green Specialty Inc, Fort Worth, TX) which provided a test specimen lot certification sheet to confirm the material pedigree, heat treatment, and certified Notched Fracture Strength (NFS) data for the

lot. Based on the NFS data, the creep frames were loaded with 325.8 lb. of dead weight at a lever ratio of 20:1 to apply the 75% NFS load per ASTM F519 specification.

11.0 Results and Discussion

11.1 NAWCWD Results

11.1.1 Dry and Wet Tape Adhesion Test Results at the NAWCWD

The results from the dry tape adhesion test on the 2L CP showed 2 out of the 3 test panels passing with an average value of 5B (Table 5). Figure 19 shows the dry tape adhesion test results, though the dry tape adhesion test for panel C shows failure of the 2L CP coating.

Table 5. Dry Tape Adhesion Test on 2L CP Coating

	Test 1	Test 2	Test 3	Minimum	Average
Dry Adhesion A	5B	5B	4B	4B	5B
Dry Adhesion B	5B	5B	4B	4B	5B
Dry Adhesion C	3B	4B	1B	1B	3B

Dry Adhesion A

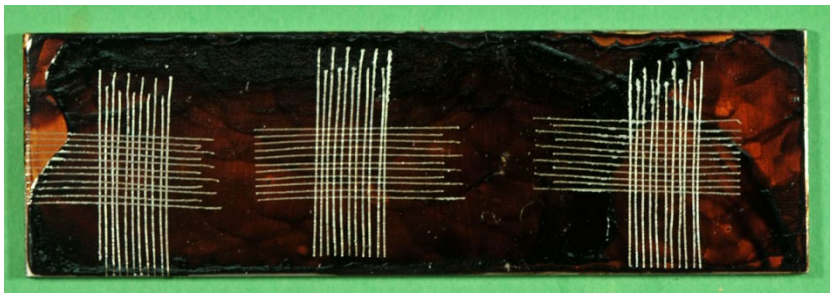

Dry Adhesion B

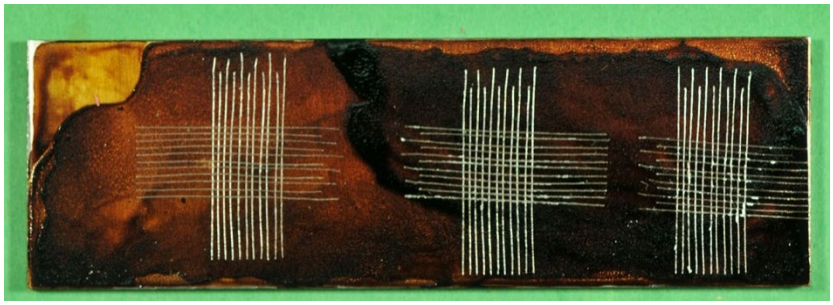

Dry Adhesion C

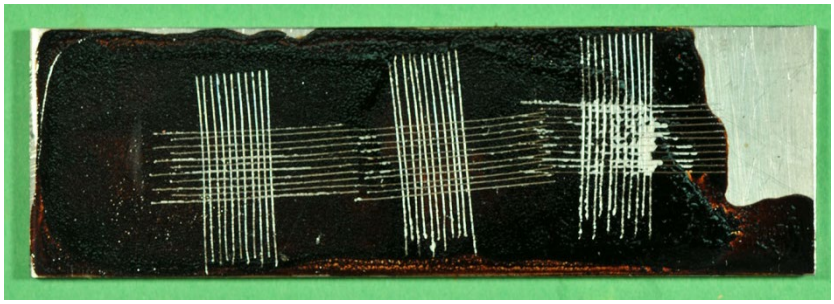

Figure 19. Panels After Dry Adhesion Tests. From top to bottom, panels A, B, and C

11.1.2 Wet Dry Tape Adhesion Test Results at the NAWCWD:

The wet tape test shows that the panels passed this test without any significant loss of the coating after exposure (Table 6 and Figure 20).

Table 6. Width of Substrate Exposure After Wet Adhesion Test

Wet Tape Adhesion	Average (in)
Wet Adhesion A	0.010
Wet Adhesion B	0.004
Wet Adhesion C	0.015

Wet Tape Adhesion A

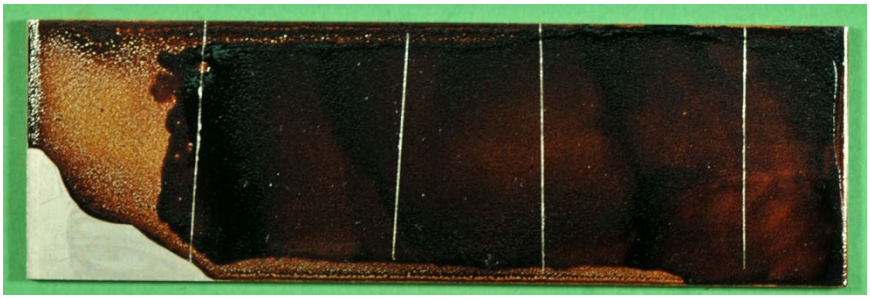

Wet Tape Adhesion B

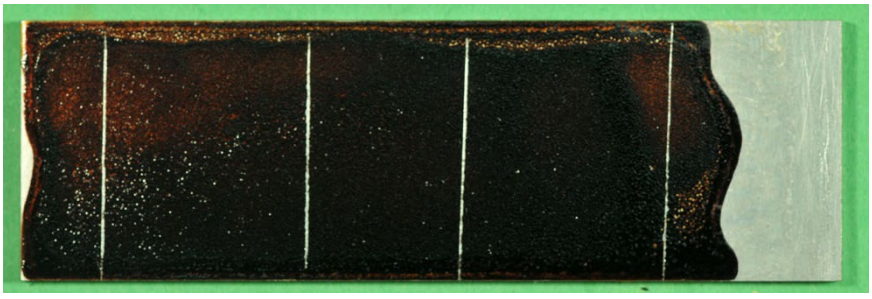

Wet Tape Adhesion C

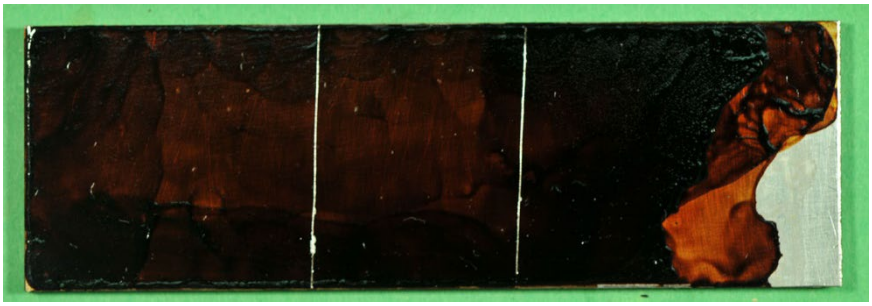

Figure 20. Panels after Wet Adhesion Tests. From top to bottom, panels A, B and C

11.1.3 Pull-off adhesion testing - Tensile Adhesion (Pneumatic Adhesion Tensile Testing Instrument (PATTI Test)) (PATTI) at the NAWCWD:

The results from the PATTI testing of the 2L polymer coating showed very high adhesive strength on the Zn-Ni CP coating (Table 7) and all tested samples demonstrated the pull-off values in the 2800 to 3300 psi range, which is indicative of very well-adhered coating material. In addition to this high tensile force data, all coating samples showed the cohesive failure that occurred predominantly in either epoxy adhesive (glue) layer or within the 2L polymer film itself (Figure 21).

Table 7. Pull-off Adhesion Test Results (PSI)

PATTI Test	Result 1	Result 2
Patti A	3220	3088
Patti B	3301	3228
Patti C	2812	No Test

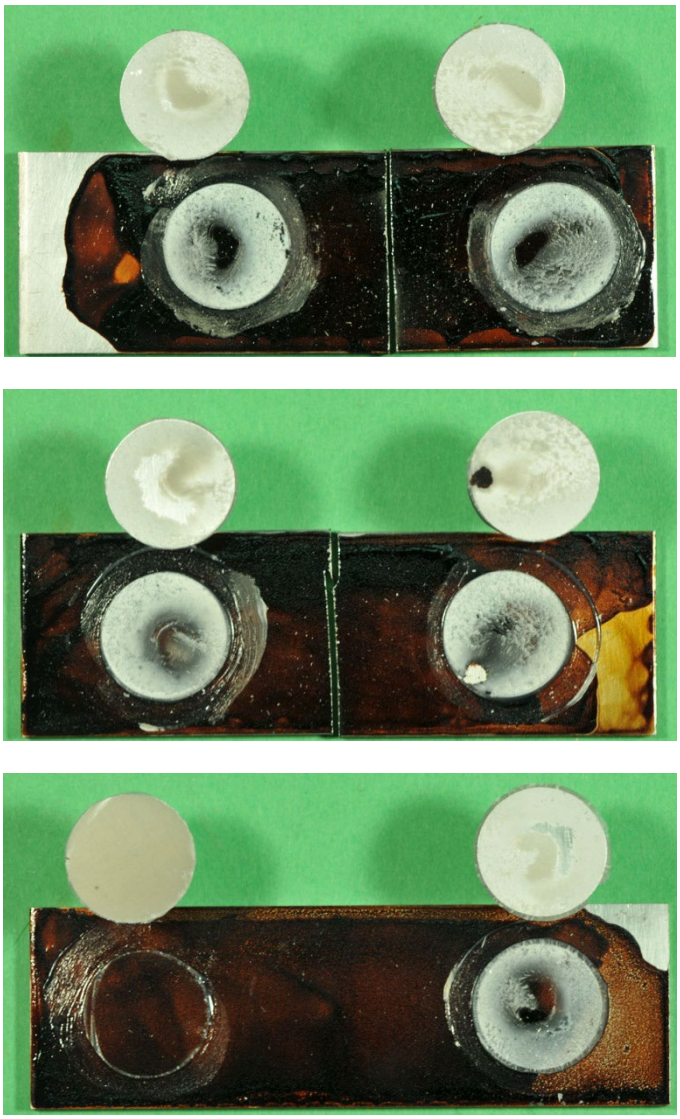

Figure 21. Panels after Pull-off Adhesion Test. From top to bottom, panels A, B, and C

Scanning Electron Microscopy (SEM) and Energy Dispersion X-ray Spectroscopy (EDS) were performed in a Zeiss Evo50. The coated face of a sample panel was examined first. Nothing remarkable was noted. Representative micrographs are in Figure 22. EDS was performed using an EDAX detector and found only carbon and oxygen. The EDS results are attached. The sample was then metallographically prepared. It was sputter coated with iridium for three cycles in order to provide a dividing line between the candidate CP coating and epoxy mounting material. After sputter coating, it was sectioned, mounted in epoxy, and polished. The candidate CP coating appeared to be unbroken. The metal plating of the panel, below the CP coating, was fractured and oddly eroded in some places. Representative micrographs are in Figure 22.

Figure 23 shows SEM images that are at 1000X and the top left image features strange degradation of metal plating. The sputtered iridium is visible as a faint line roughly 20 microns

from the plating. Bright areas beyond that line are the result of the sample charging and top right image is the same field of view, but created using a different detector. The bottom left image is a different field of view and it again shows the iridium coating and charging beyond that. The bottom right image is the same as bottom left, and shows that the CP coating is intact.

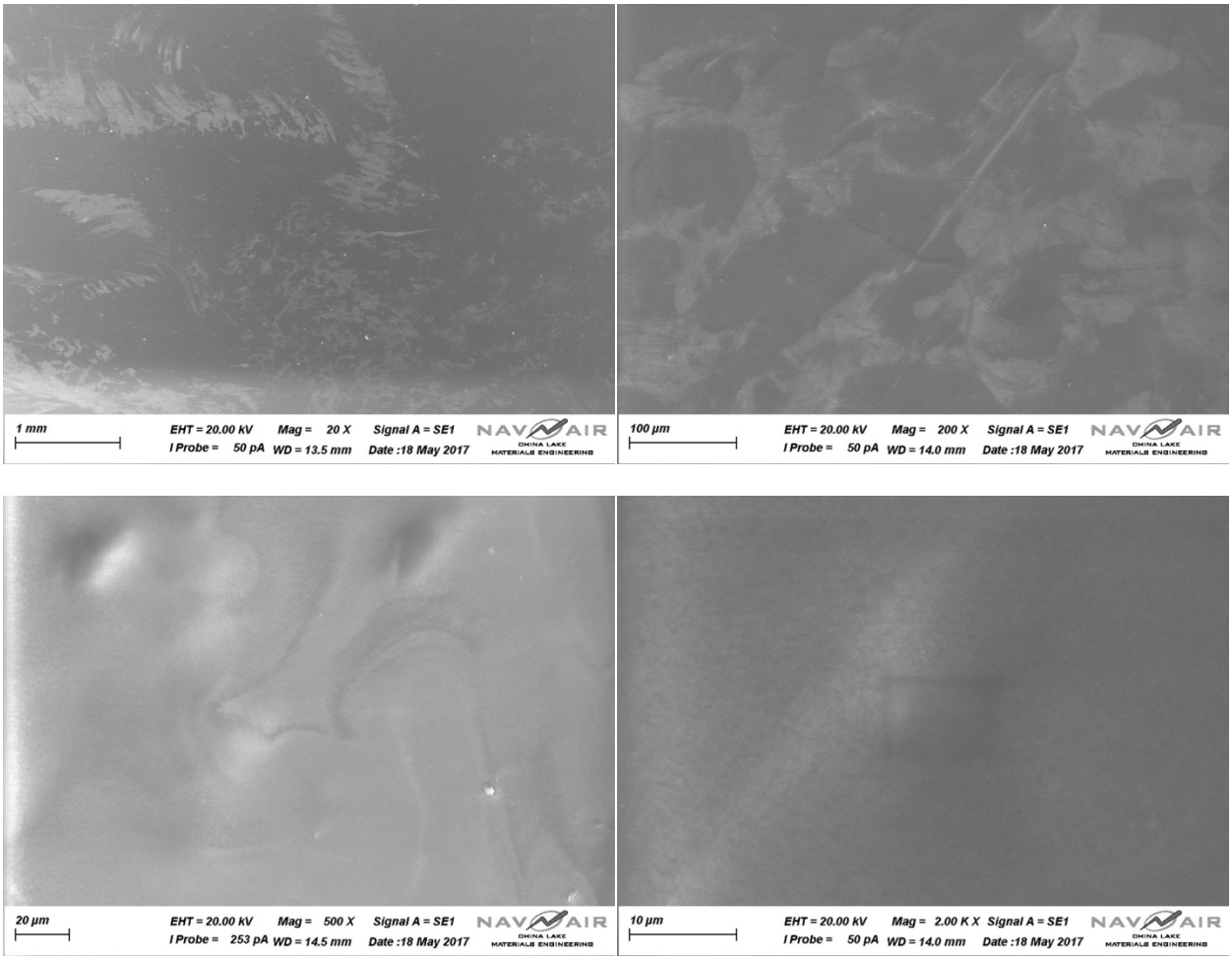

Figure 22. Representative Micrographs of Candidate Coating Face. Images are at 20X, 200X, 500X and 2000X magnification

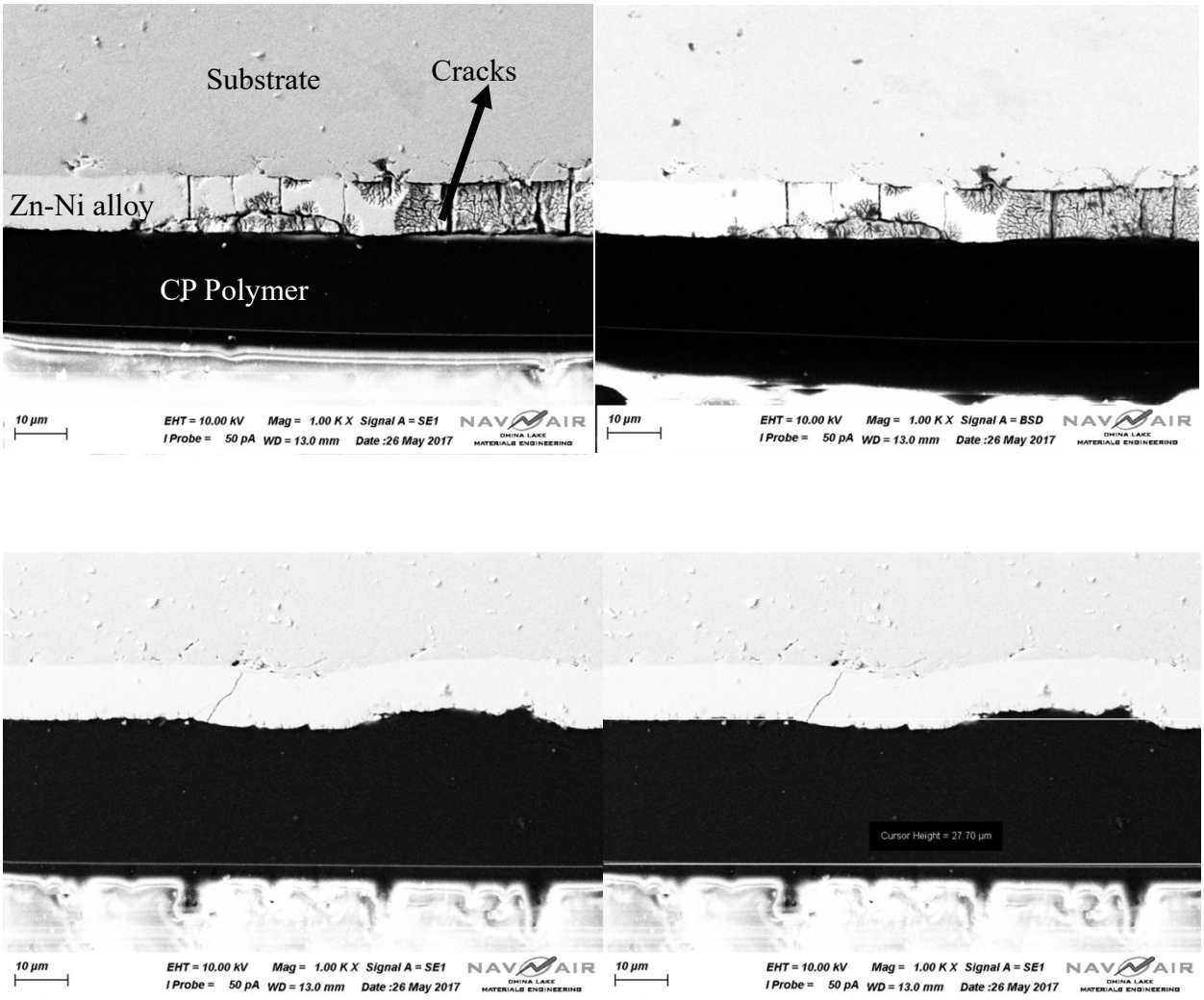

Figure 23. Representative Micrographs of Sectioned Candidate Coatings
(Upper left labelled figure with coatings)

11.1.4 NSS test results on CP coated Zn-Ni coated high strength steel coupons at the NAWCWD:

The results of the NSS results are shown in Figure 24. The bulk of the coating remained intact and adhered to the substrate. Blistering of the coating is evident but the underlying Zn-Ni coating did not appear to show extensive corrosive products. After this, it was noted that when the coating was removed, there did not appear to be stereotypical corrosion. The panel had blistered during exposure to the NSS exposure. These blisters of the CP coating were easy to remove by scraping. In areas without blistering the coating remained steadfastly adhered. Photographs were taken of the panel with some coating removed. One photograph is in Figure 25 and the coloration reminiscent of tree rings are visible where the blister evidently grew. It was believed that this

would show a gradient of corrosion product, with minimal product near the edge of the scraping. The elements present were zinc, oxygen, carbon, copper, and chlorine. The copper is localized to a band of copper tape, deliberately included to provide contrast. The zinc is localized to the exposed region, and the carbon to the coated region, as would be expected. The oxygen is evenly distributed throughout the sample, which shows that there is not the expected varying concentration of corrosion, in agreement with what was indicated by earlier EDS runs. The chlorine is localized to the area with substrate exposed. To further investigate, it was preferable to remove the coating fully. On a selected panel that had not been exposed to salt fog a variety of methods were employed, none successful. The first method was scraping, followed by exposure to an industrial paint stripper, Mentor 404, containing D-limonene and N-methyl-pyrrolidine for five minutes, followed by scraping. Then acetone immersion was tried for five minutes, again followed by scraping another method was the use of industrial paint stripper, Jasco Premium Paint and Epoxy Remover, containing principally methylene chloride, for fifteen minutes. An attempt using nitromethane for five minutes was attempted without success. Finally, MEK was used, for five minutes and again, none of these solvents were effective. Without being able to remove the coating, a comparable panel was used, one with some of the surface uncoated. This panel is pictured in Figure 26. The uncoated portion was observed under SEM and EDS showed a lower concentration of oxygen (4-5 wt.%) on the substrate than on the corroded substrate (16-22 wt.%).

Some of the scrapings were kept from the blistered panel. It was noted that there were light colored markings on the underside of the coating. A scraping of coating was loaded into the Evo50 SEM. High magnification revealed crystals on the coating. Examples are in Figure 27. EDS showed that the composition of the crystals is zinc, oxygen, and chlorine. Several localized EDS scans were performed, showing that the zinc and chlorine were localized to the crystals.

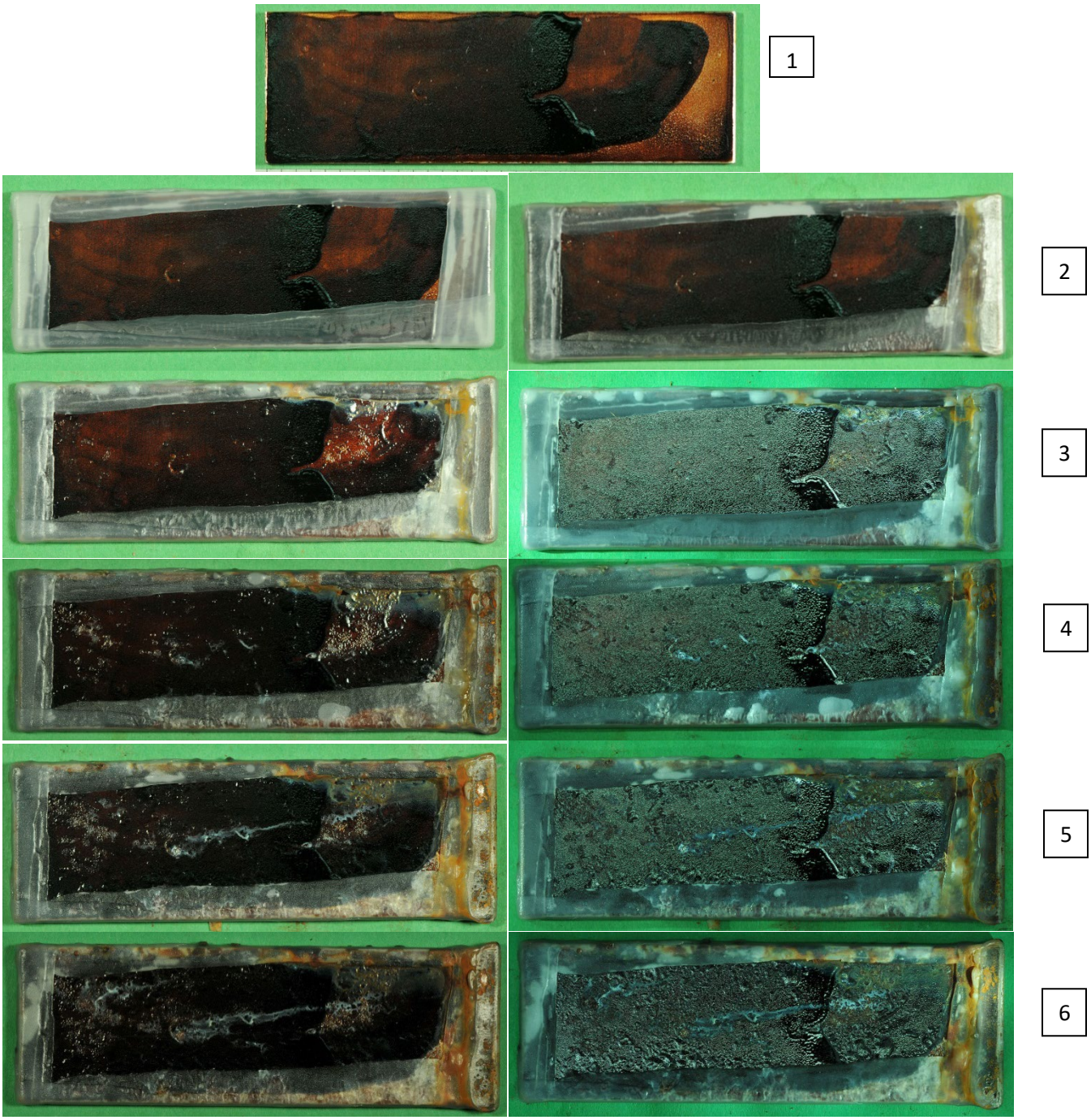

Figure 24. Representative Panel NSS During Salt Fog Testing. Row 1: before testing. Row 2, left: before testing with wax. Row 2, right: after 100 hours testing. Row 3: after 200 hours; right image is with intense side lighting. Row 4: after 300 hours. Row 5: after 400 hours. Row 6: after 500 hours. Images are representative of all test samples

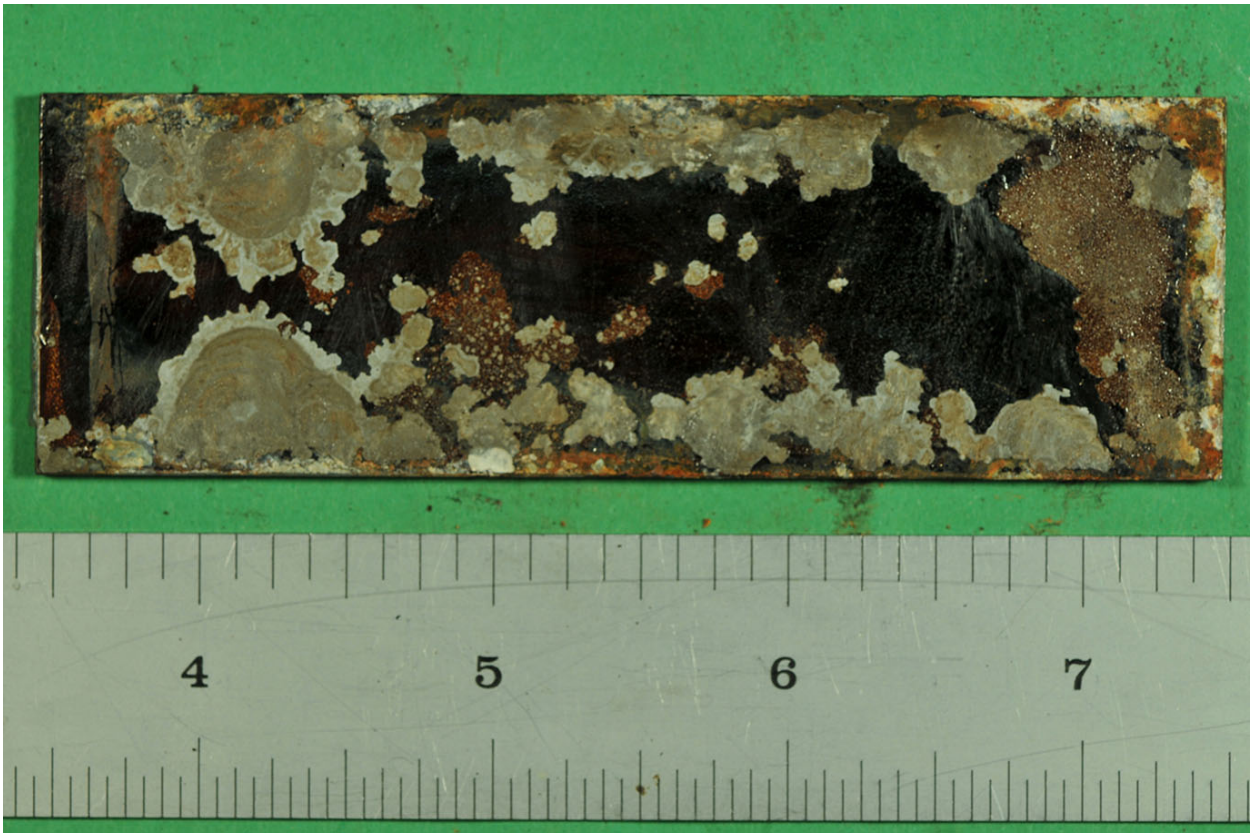

Figure 25. Panel after salt fog chamber with blistered coating removed

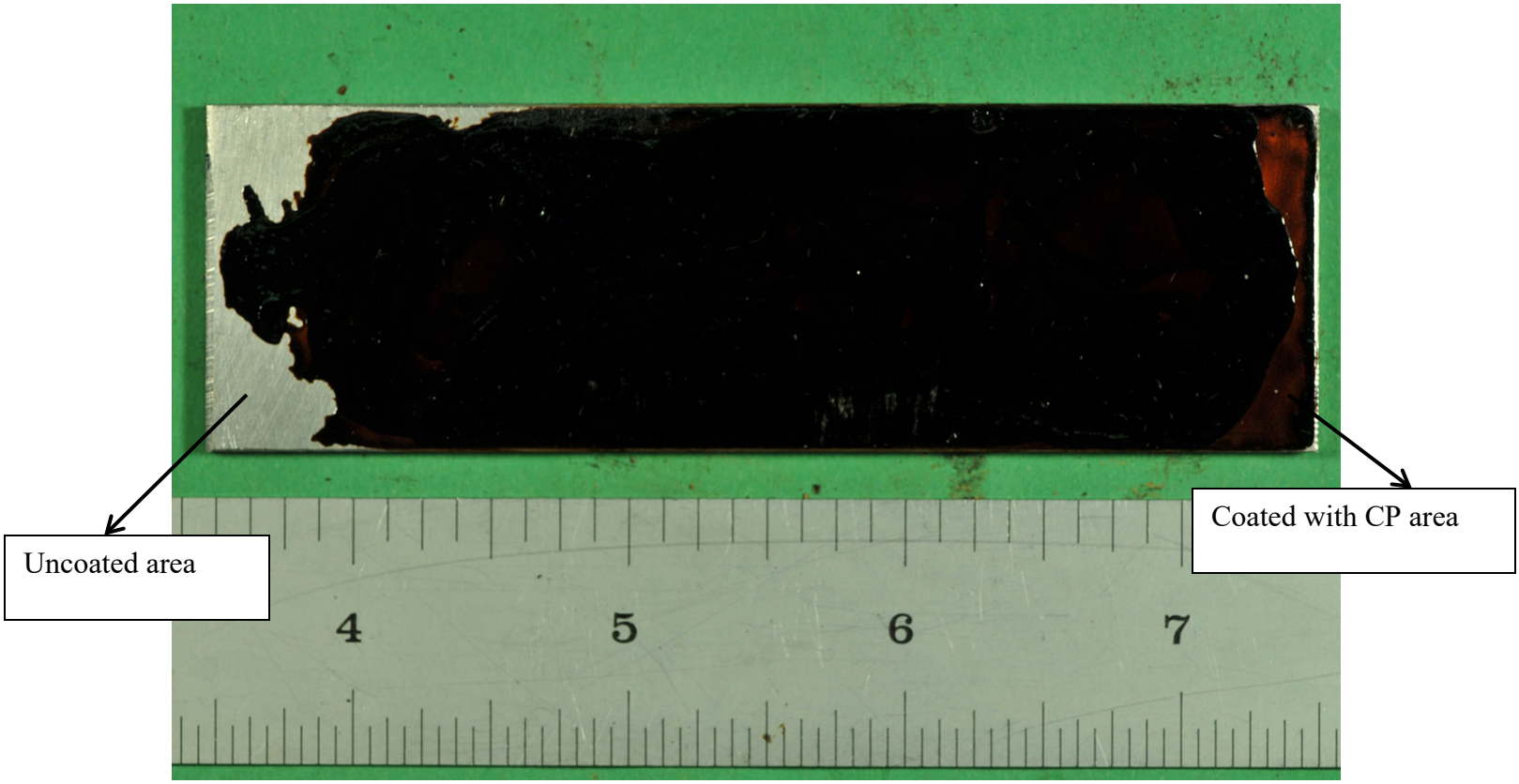

Figure 26. A panel comparable to those exposed to salt fog, unexposed. The uncoated surface served as a baseline when coating could not be removed

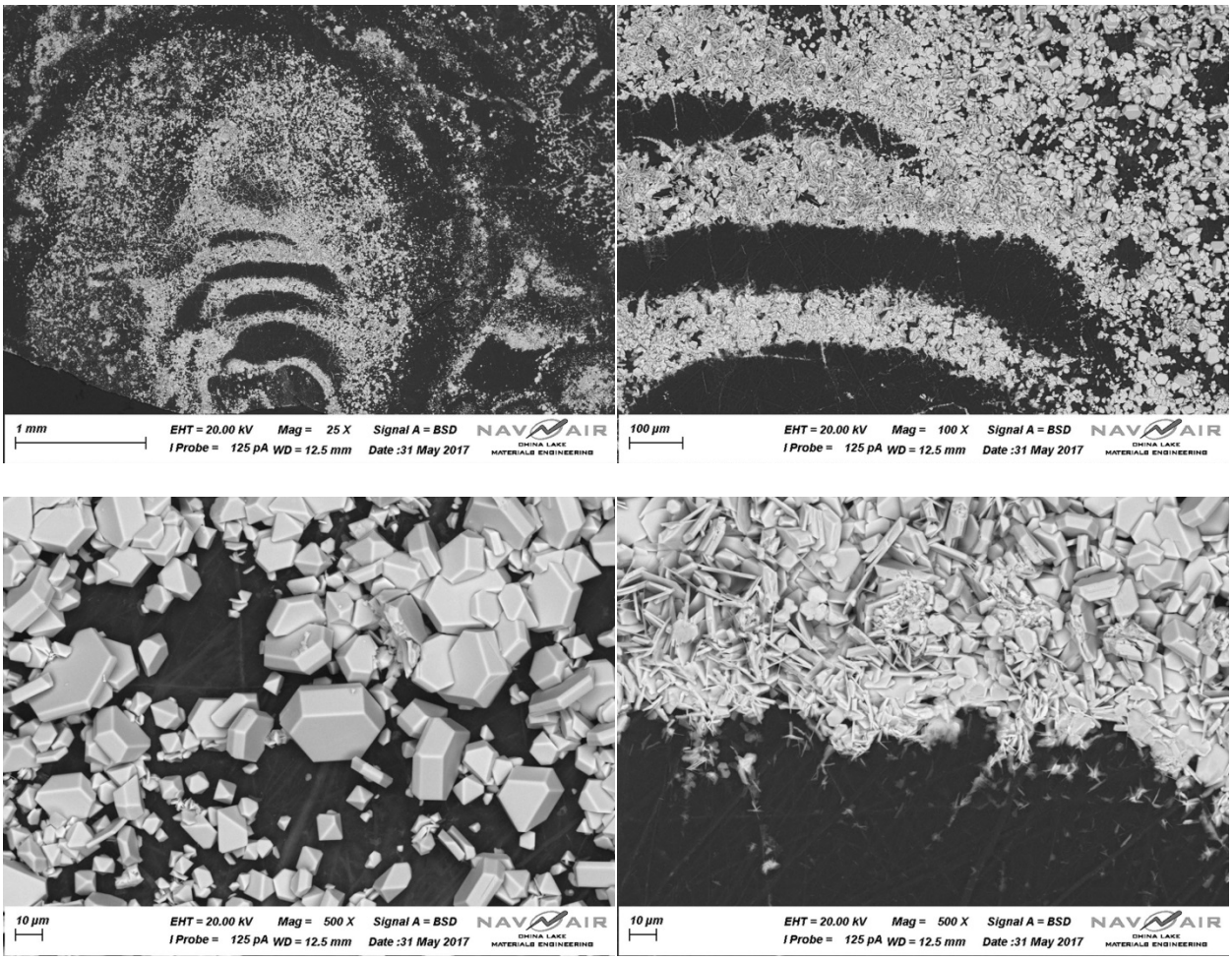

Figure 27. Crystals composed of zinc, oxygen, and chloride from the underside of a CP panel coating

A further examination for the possibly of corrosion underneath the CP coating was investigated, via an X-ray cabinet, then by eddy current for coating thickness, and finally via a tap test. The X-ray cabinet revealed nothing and a representative image is shown Figure 29. Coating thickness measurements using the Delfelsko Positector 6000 Eddy Current analyzer were inconclusive as well. The measurement locations are detailed in Figure 30. The measured thicknesses are in Table 8. The region of possible corrosion is number 4, which was actually measured thinner than other areas. The tap test was inconclusive as well; the pitch changed as a function of location (due to edge effects) to a degree that made any indication of subsurface corrosion unnoticeable.

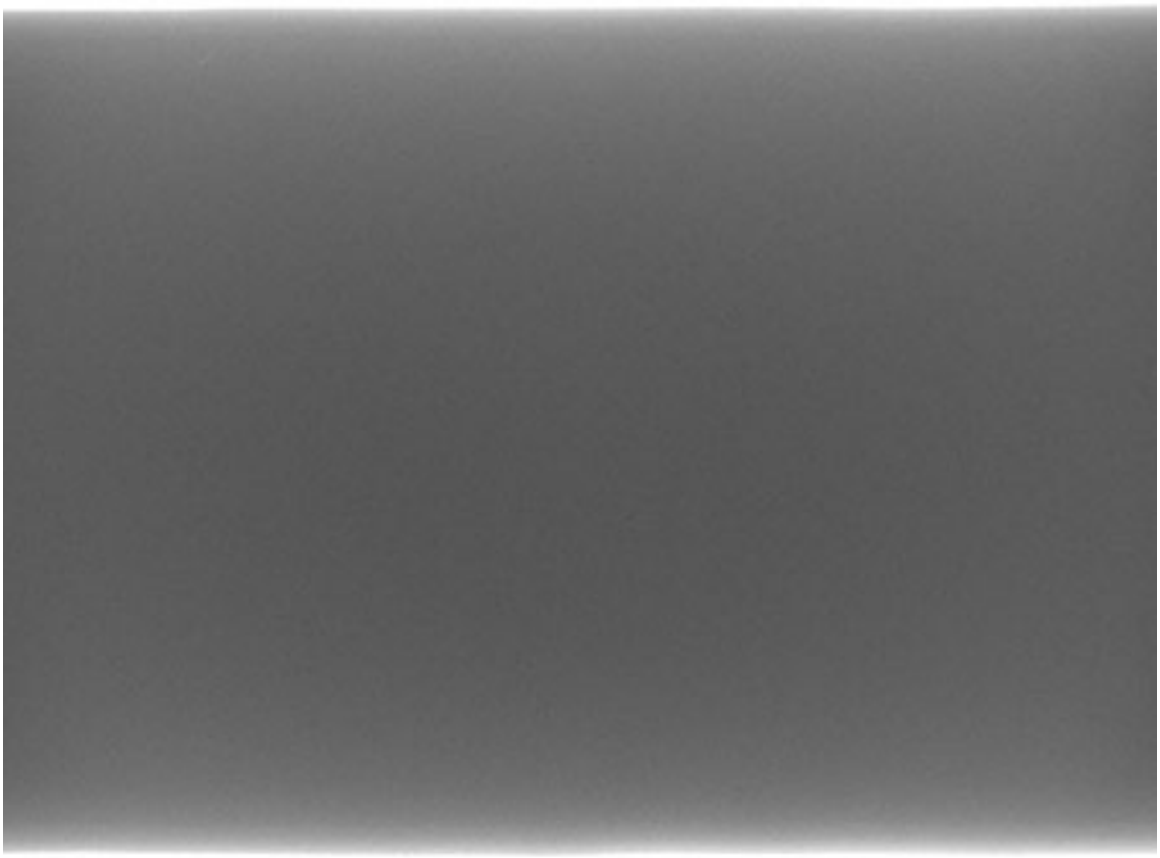

Figure 28. Panel as viewed in the X-ray cabinet

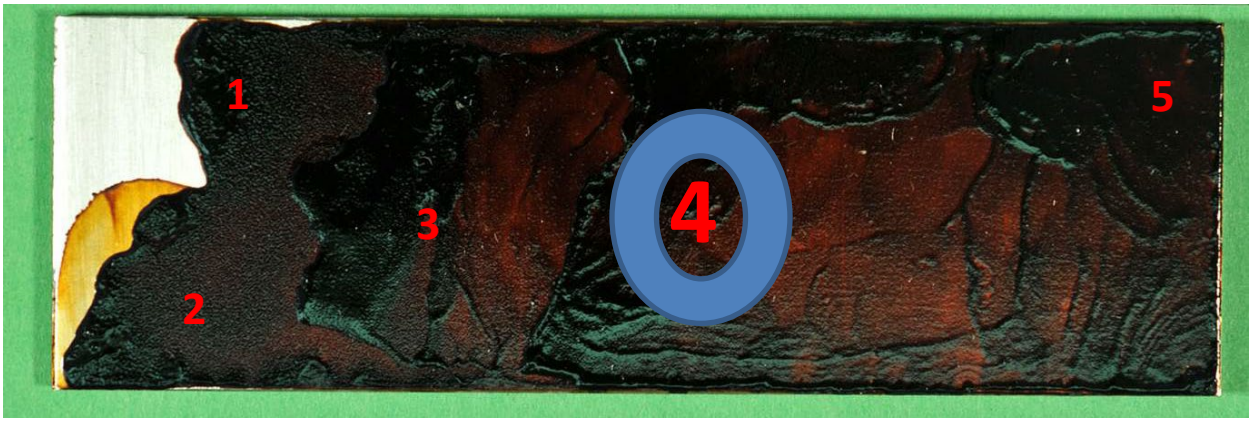

Figure 29. Panel with possible corrosion and locations of coating thickness measurements

Table 8. Coating Thickness Measurements of Panel with Possible Sub-coating Corrosion (mils)

Location	Average
1	1.63
2	1.23
3	2.43
4	0.98
5	1.40

11.1.5 Contact Resistance Measurements at the NAWCWD:

The resistivity of the CP films was measured before and after NSS exposure. This property will determine if the 2L CP film complies with the contact resistance requirements specified in MIL-DTL 38999L, Class Z. The 2-layer polymer films were completely insulating immediately following the 2L CP coating and after exposure to NSS for 500 hours the measured value was 6±2 MΩ. Electrical connectors employing these technologies should have a consistent shell-to-shell contact resistance of <2.5mΩ before, and <5mΩ after corrosion testing, as required by MIL-DTL-38999L, Class Z, Section 3.29. Our results fell outside this range and did not meet this specific requirement as stated in the mil spec.

11.2 WFAB/UDRI Results

11.2.1 Characterization of Coating Thickness and Morphology at WAFB/UDRI

Though DFT gauge is considered to be ideal for measuring non-magnetic and non-conductive coatings over steel or other metal, it was found also suitable to measure the thickness of the NAWCWD CP films on steel substrate, probably due to a significant difference in electrical conductivity between the metal substrate and the CP material. Table 9 shows the results of measuring the DFTs of the conductive polymer coatings obtained for both groups of samples using PosiTector 6000 gauge equipped with combination magnetic/eddy current probe. As evident from the relatively large standard deviation values, the coating thickness is not uniform. This is also quite noticeable visually; with some areas of the coated samples appear much darker indicating thicker coating in that area.

Table 9. Dry Film Thickness Data Obtained via DFT Gauge

Coating	Dry Film Thickness, mils
1L	0.12±0.03
2L	1.45±0.17

An examination of film morphology on conductive polymer coating samples was conducted using scanning electron microscopy (SEM) technique. The imaging was performed using the Hitachi TM3000 tabletop SEM microscope with a backscattered detector at 15 kV operating voltage and variable magnification. The SEM technique was also used to determine the coating thickness via a cross-sectional imaging of the coating. For the cross-sectional view of the coating, the sample preparation was done by a mechanical fracturing of the coated substrate. For this purpose, a piece of Zn-Ni-plated steel coated with the conductive polymer was undercut from the uncoated side using a low-speed diamond saw and then sharply bent along the cut in order to exposure the layered structure. The SEM images of the coating sample shown below illustrate both typical defects of the solution-casted coating (top view images) and the morphology of the film adhered to Zn-Ni-coated steel substrate (cross-sectional or side view). For the 1L coating samples, the top-view SEM images shown in the Figure 30 revealed two types of defects visible on the surface of the coating: the small circular crater-like cavities formed probably from the evaporated solvent during casting of the film and the multiple cracks going through the coating material. The cross-sectional view of 1L coating (Figure 31) shows dark coating lying on top of

light-colored Zn-Ni plated layer; the steel substrate appears underneath as a dark-grey colored layer. The film thickness of 1L conductive polymer coating was estimated to be in 5-7 micrometer range. However, in the case of 1L coating samples, it was difficult to accurately perform a cross-sectional sample preparation and SEM imaging due to a relatively weak adhesion of thin polymer coating and its easy smearing along the edges of the fractured sample. For the 2L coating samples, the SEM imaging reveal the uniform and defect-free coatings observed in both top-view (Figure 32) and cross-sectional view (Figure 33) images. One of the top-view images shows the ripples visible on the film surface. Those ripple defects are also visible by the naked eye on a larger scale as an orange peel defects developed on the coated surface. Both types of defects – either small-scale pits and micro-cracks observed for 1L coating samples, or large-scale "orange peel" ripples of the 2L coating samples – are probably inherent to the drop-casting method of the coating application and can be eliminated once the application process is optimized. The cross-sectional SEM image of the Figure 33 shows the 2L polymer coating positioned on top of light-colored Zn-Ni electroplated layer with approximately 13 μm in thickness and the steel substrate is visible underneath of this layer. The film thickness of the polymer coating is estimated to be in 15-20 micrometer range. The additional images of the 2L coating samples are provided in Figure 34.

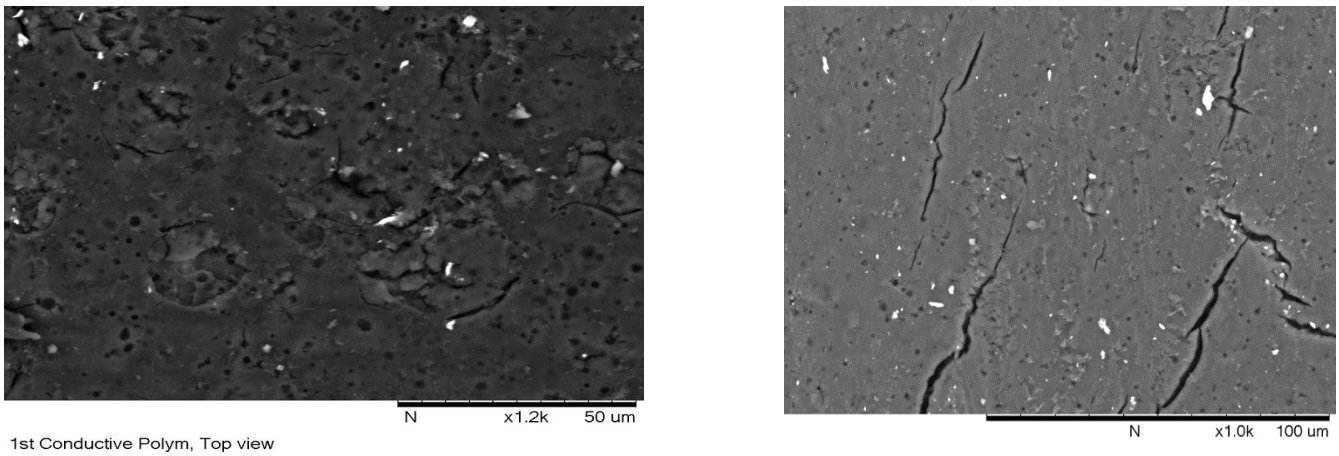

Figure 30. Top-view SEM Images of 1L Conductive Polymer Coating

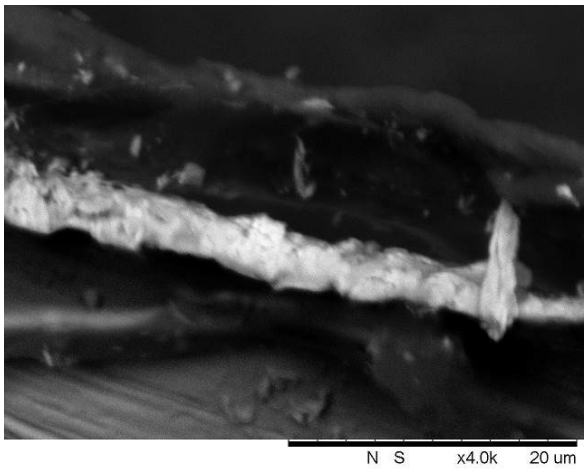

Figure 31. Cross-sectional or Side-view SEM Image of 1L Conductive Polymer Coating

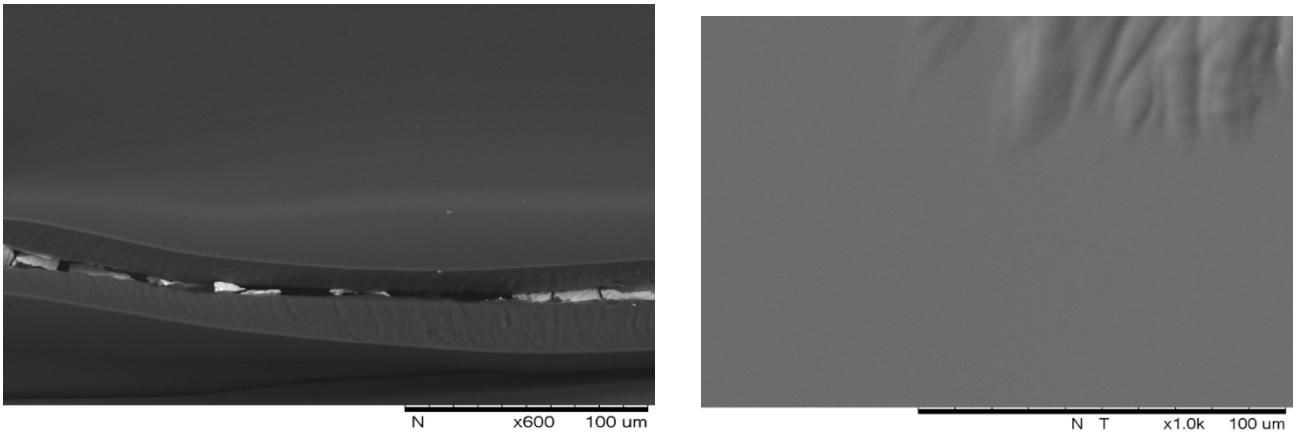

Figure 32. Top-View SEM Images of 2L Conductive Polymer Coating

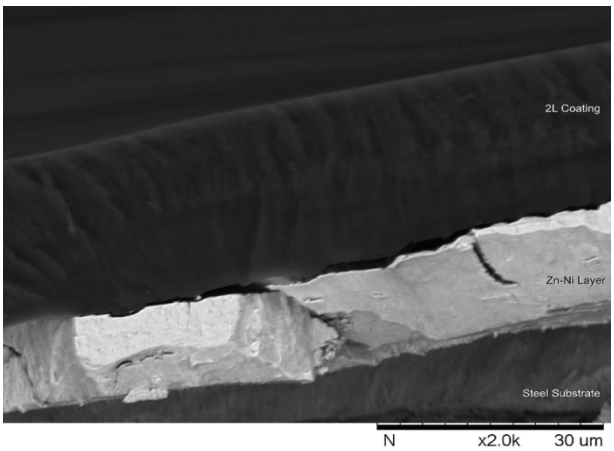

Figure 33. Cross-Sectional or Side-View SEM Image of 2L Conductive Polymer Coating

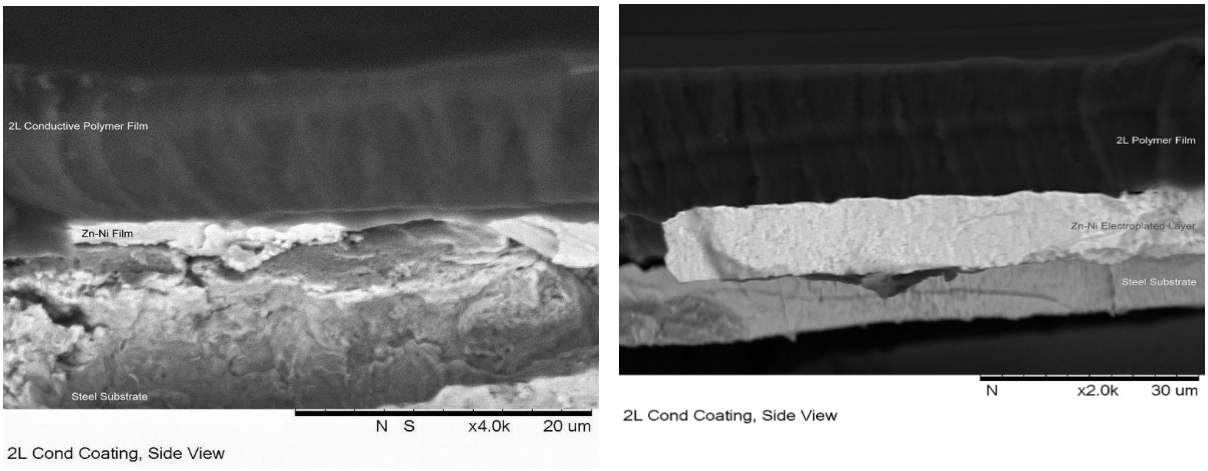

Figure 34. Side-view SEM Image of 2L CP coating

11.2.2 Dry and Wet Tape Adhesion Testing at WPAFB/UDRI

Both the 1L and 2L CP coating samples were tested for dry tape adhesion in accordance with ASTM D3359 (Standard Test Methods for Measuring Adhesion by Tape Test; Method B). A crosshatch pattern was scribed through coating down to the substrate. A strip of 1-inch-wide masking tape, such as 3M 250 or equivalent was applied. The tape was pressed down using two passes of a 4.5-pound rubber covered roller. The tape was removed in one abrupt motion perpendicular to the panel. The adhesion was rated by a visual examination of the paint at the crosshatch-scribed area using the ASTM provided rating system.

For wet tape adhesion testing, the uncoated surface of the steel coupons was masked off using electroplating tape in order to prevent corrosion of steel substrate. The panels were immersed in de-ionized water for 24 hours at room temperature. After immersion, the samples were dried and allowed to sit at ambient conditions for 3 minutes. A crosshatch pattern was scribed through coating down to the substrate. A strip of 1-inch-wide masking tape, such as 3M 250 or equivalent was applied. The tape was pressed down using two passes of a 4.5-pound rubber covered roller. The tape was removed in one abrupt motion perpendicular to the panel. The adhesion was rated by a visual examination of the paint at the crosshatch-scribed area using the rating scale in ASTM D 3359 Method B. The testing was performed in triplicates. Test data for both wet and dry tape adhesion testing for 1L coating samples is shown in Table 10. Figure 35 shows the images of the cross-hatch scribed area of the samples after the adhesive tape was applied to them. The images illustrate the peel-off effect of the adhesive tape on coating samples subjected to either dry or wet conditions. The additional images of 1L coating samples are shown in Figure 36.

Table 10. Dry and Wet Tape Tests for 1L CP Coating

Adhesion Test Type	Panel ID	Method B Rating	Area Removed, %
Dry Tape	1L-3 DT	4B	Less than 5%
	1L-10 DT	4B	Less than 5%
	1L-15 DT	4B	Less than 5%
Wet Tape	1L-8 WT	0B	More than 65%
	1L-19 WT	0B	More than 65%
	1L-22 WT	0B	More than 65%

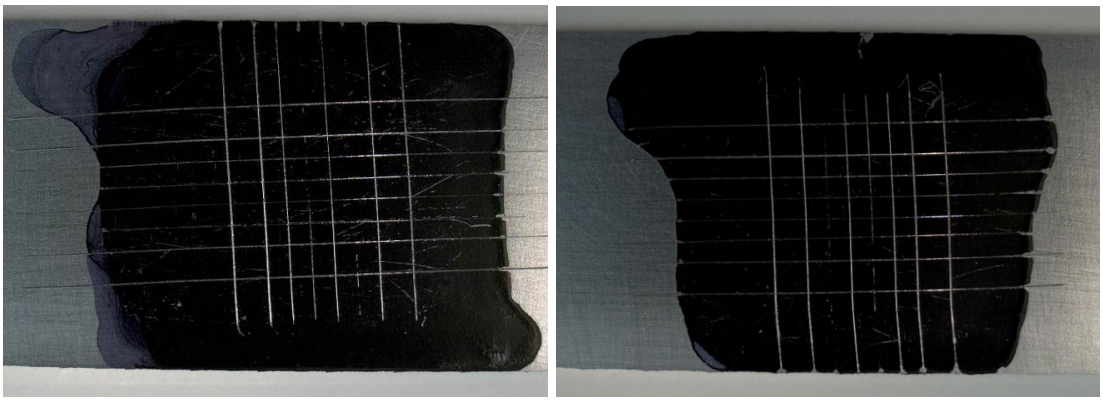

Figure 35. Dry Tape Test Results for 1L CP Coating

Figure 36. Wet Tape Test for 1L CP Coating

As it is clear from the comparison of the dry and wet tape test results (Figure 37), the adhesive strength of the coating was substantially diminished after the samples were exposed to water. The visual estimation indicates that more than 65% of coating was removed from the surface of the

substrate after the samples were exposed to water. Dry tape adhesion evaluation showed less than 5% loss of the coating material or 4B rating.

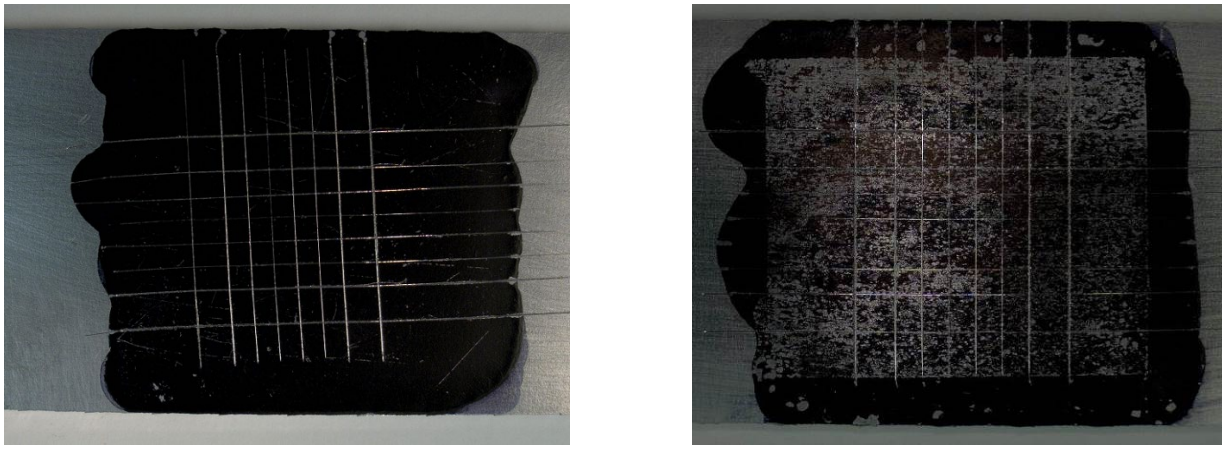

Figure 37. Representative Images of 1L Coating Samples after Dry Tape (left) and Wet Tape (right) Tests

Table 11 shows the results for both wet and dry tape adhesion testing summarized for the 2L coating samples. The images of the actual tested 2L samples are shown in Figure 38, and the images were taken after the samples were scribed with a cross-hatch pattern and the adhesive tape was applied to them. The images illustrate the peel-off effect of the adhesive tape on coating samples subjected to either dry or wet conditions. As it is clear from both the rating data and the images, the adhesion of all 2L samples tested in dry or wet conditions was quite good. In the worst case of 4B rating, only negligible amount of coating material was removed around the scribed lines and the edges of the cross-hatch pattern. The samples performed equally well in both dry and wet testing conditions. Additionally, 2L coatings showed substantially improved adhesion in wet conditions, as compared to 1L coatings that showed almost complete loss of the coating material after water exposure and failed in wet tape testing.

Table 11. Dry and Wet Tape Adhesion Testing Data for 2L Coatings

Adhesion Test Type	Panel ID	Method B Rating	Area Removed, %
Dry Tape	2L-1 DT	5B	0%
	2L-2 DT	4B	Less than 5%
	2L-3 DT	4B	Less than 5%
Wet Tape	2L-1 WT	4B	Less than 5%
	2L-2 WT	4B	Less than 5%
	2L-3 WT	4B	Less than 5%

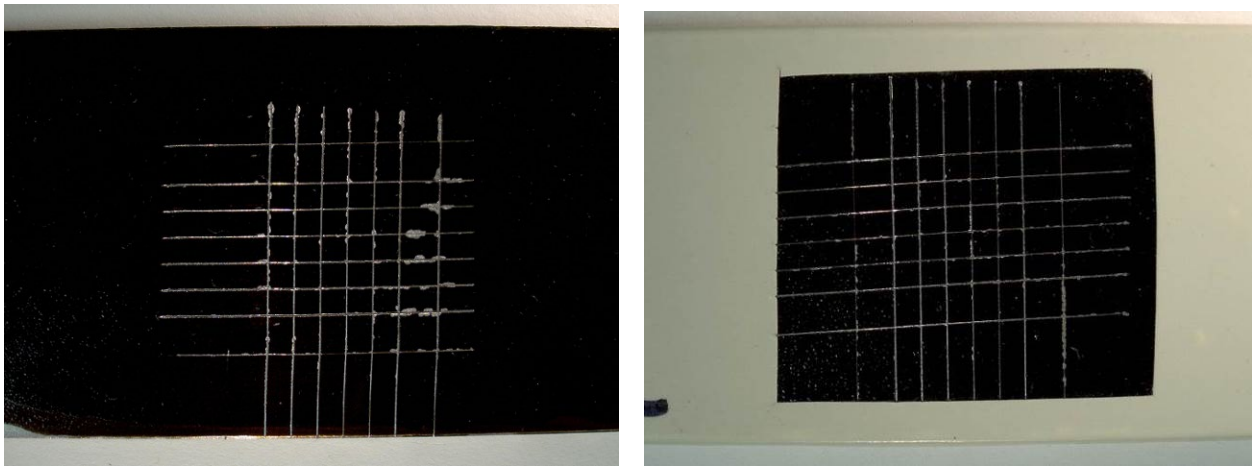

Figure 38. Representative Images of 2L Coating Samples after Dry Tape (left) and Wet Tape (right) Tests

11.2.3 Tensile Adhesion (PATTI) Testing at WPAFB/UDRI

The Pneumatic Adhesion Tensile Testing Instrument (PATTI) uses a compressed air system to determine an adhesive strength by pulling a pre-attached stub from the coating surface (see Figure 39 as illustration). The PATTI test is considered quantitative as it is based upon the tensile strength values obtained from the experiment. Data from the PATTI adhesion testing of 1L and 2L conductive polymer coatings is shown in Table 12. The adhesion data can be evaluated based on a comparative analysis of the tensile strength data and the character of failure observed during the test. In general, the PATTI data demonstrates of how much tensile force can be applied to the surface of a coating before either adhesive or cohesive failure can occur. Failures can be either adhesive (between the interfacial layers - e.g., between the substrate and the coating layer) or cohesive (e.g., within the coating layer). In the case of 1L conductive polymer coating samples, the primary mode of failure is well defined, which is an adhesive failure at the coating/substrate

interface. Visually (see Figure 39), it resulted in almost complete transfer of black polymer film from Zn-Ni plated steel substrate to the epoxy adhesive on the surface of the stud. In addition to the primary adhesive failure, a very small amount (less than 5% of total surface area of the stud) of Zn-Ni plated material was observed as minor greyish speckles on a stud surface. These Zn-based material transfer is visible on shown magnified optical microscopy images (Figure 40) illustrating the fact of very minor cohesive failure within Zn-Ni plated layer. It is not clear if this happened due to abrasive surface preparation of substrate panels before the coating application or due to the mechanical properties of electro-plated Zn-Ni material.

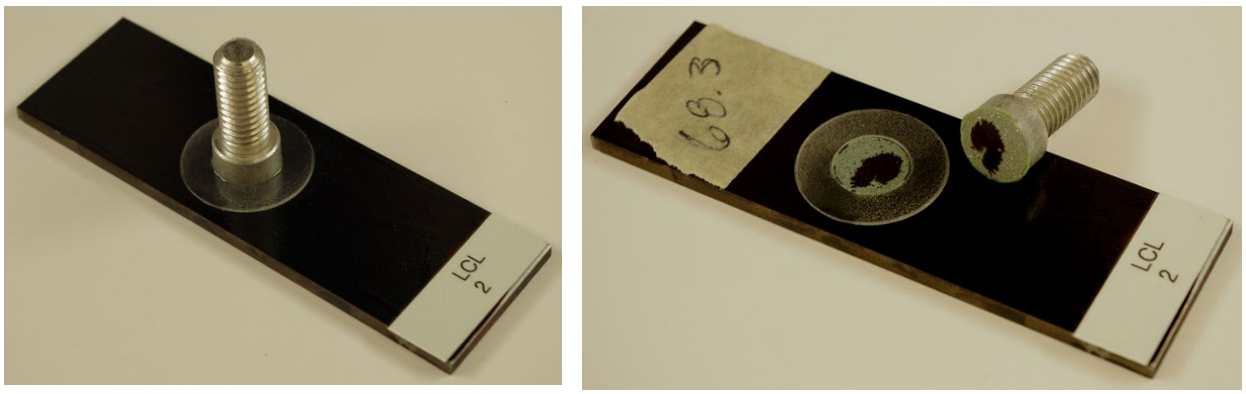

Figure 39. Example of a 1L coated sample before and after PATTI test

Table 12. PATTI Adhesion Testing Data for Both 1L and 2L Coatings

Panel ID	Gage Pull-Off Pressure, psig	Calculated psi	Average of Calculated psi	Primary Failure Mode
1L-1	12.5	505	566±63	Coating/Substrate Adhesion
1L-2	13.9	562		Coating/Substrate Adhesion
1L-3	15.6	631		Coating/Substrate Adhesion
2L-1	52.2	2125	2339±344	Glue Failure/Coating Cohesion
2L-2	68.3	2782		Glue Failure/Coating Cohesion
2L-3	65.1	2652		Glue Failure/Coating Cohesion
2L-4	56.6	2305		Glue Failure/Coating Cohesion
2L-5	45.2	1859		Glue Failure/Coating Cohesion
2L-6	57.3	2333		Glue Failure/Coating Cohesion

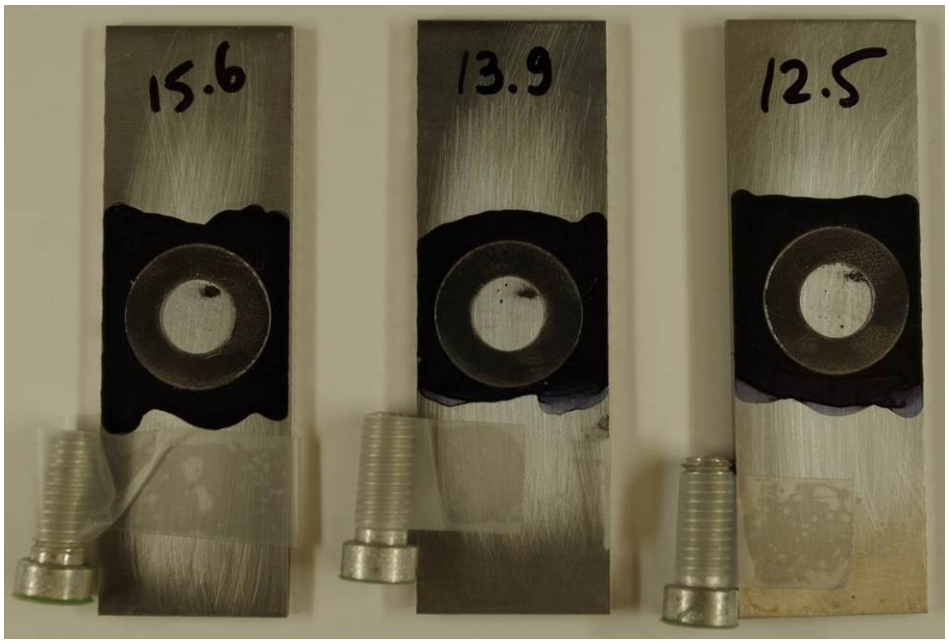

Figure 40. Images of 1L Coating Samples after PATTI Test

In addition to the primary adhesive failure, a very small amount (less than 5% of total surface area of the stud) of Zn-Ni plated material was observed as minor greyish speckles on a stud surface. These Zn-Ni based material transfer is visible on shown magnified optical microscopy images (Figure 41) illustrating the fact of very minor cohesive failure within Zn-Ni plated layer. It is not clear if this happened due to abrasive surface preparation of substrate panels before the coating application or due to the mechanical properties of electro-plated Zn-Ni material.

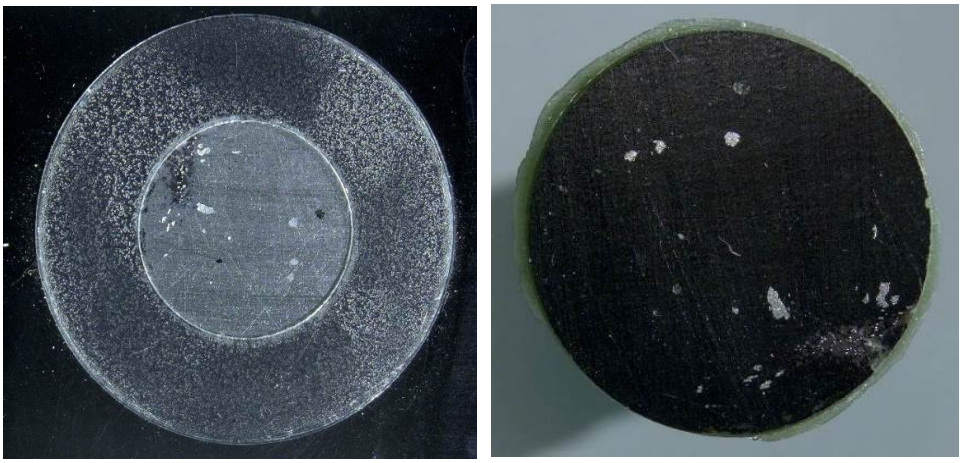

Figure 41. Images of 1L Coating after PATTI Test: Substrate (left) and Stud (right) Surfaces

In comparison to 1L coating samples, 2L coatings demonstrated greatly improved pull-off values and the different mechanism of failure which was indicative of good coating-to-substrate

adhesion. All tested samples demonstrated the pull-off values in the 1900 to 2800 psi range, which is indicative of well-adhered coating material. In addition to this high tensile force data, all coating samples showed the cohesive failure that occurred predominantly in either epoxy adhesive (glue) layer or within the 2L polymer film itself. In several of the tested samples, the cohesive failure within the Zn-Ni electroplated layer was observed. The example of this type cohesive failure is shown in the Figure 42, where the approximately 10% of the surface of the separated stud is covered with flakes of greyish Zn-based metal coating. In contrast to 1L coating samples, none of the 2L tested samples showed any adhesive failure at the coating/substrate interface, which confirms the ability of this polymer material to form a well-adhered coating on Zn-Ni-electroplated steel substrate.

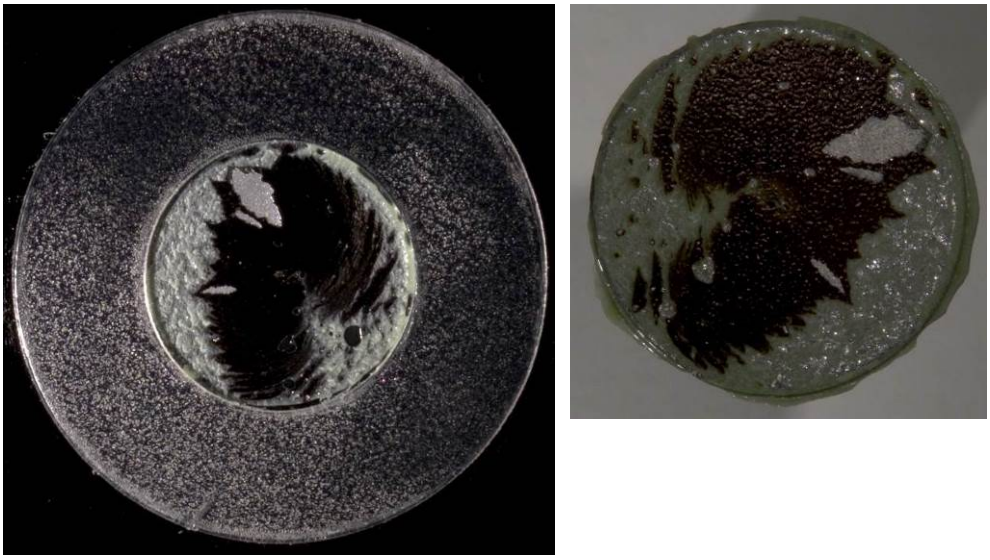

Figure 42. Images of 2L Coating after PATTI Test: Substrate (left) and Stud (right) Surfaces

11.2.4 Accelerated Corrosion by Neutral Salt Spray (NSS) Testing at WPAFB/UDRI

The accelerated corrosion testing of the conductive polymer coating samples was performed in accordance with ASTM B 117 using 5% (by weight) sodium chloride solution with neutral (~7) pH. Sometimes, this salt spray test is also called as neutral salt spray (NSS) test. The basis for the testing criteria was the visual examination of the samples conducted at 100 h increments of exposure for the signs of blistering, coating delamination, or corrosion spots. Before the visual examinations, the exposed panels were thoroughly rinsed with tap/de-ionized water and then dried. The images of the representative coating sample shown in Figure 43 illustrate the progression of the corrosive degradation developed upon the salt spray exposure of 1L conductive coating samples. After the initial 100 h of salt spray exposure, the coating is already failing which is evident by the appearance of whitish corrosion product on the sample surface. This is indicative of the initial corrosion of under-laying zinc-rich plating material. As the exposure progresses to

200 h, the corrosion of deeper laying steel substrate becomes visible with multiple spots of rust (iron oxide) appeared on the surface of the sample. The black polymer coating is still visible between the areas of rust, when the sample is wet. In conclusion, despite some polymer film is still adhering to the substrate surface after 200 h of exposure, the overall corrosion protection of these 1L coatings and resistance to salt spray exposure is very limited since in a relatively short time the obvious signs of corrosion are starting to develop on the sample surface. In contrast to 1L conductive coatings, 2L coatings exhibited greatly improved corrosion resistance behavior at the conditions of the NSS testing. The images of the representative 2L coating sample shown in Figure 44 illustrate the progressive effect of salt spray exposure on 2L coating samples. Though after 200 h of NSS exposure the majority of 2L coating samples started to show some initial blistering and coating lifting, there was no sign of coating rupture and the corrosion developing through the polymer film. After 500-600 h on NSS exposure, only one sample out of 5 tested showed minor ruptures of the coating with spots of rust coming from the underlying steel substrate and appeared on the surface. For the rest of the tested samples, the coating barrier was still intact after 500 h of exposure though with noticeable signs of blistering developing over the exposed area of the sample.

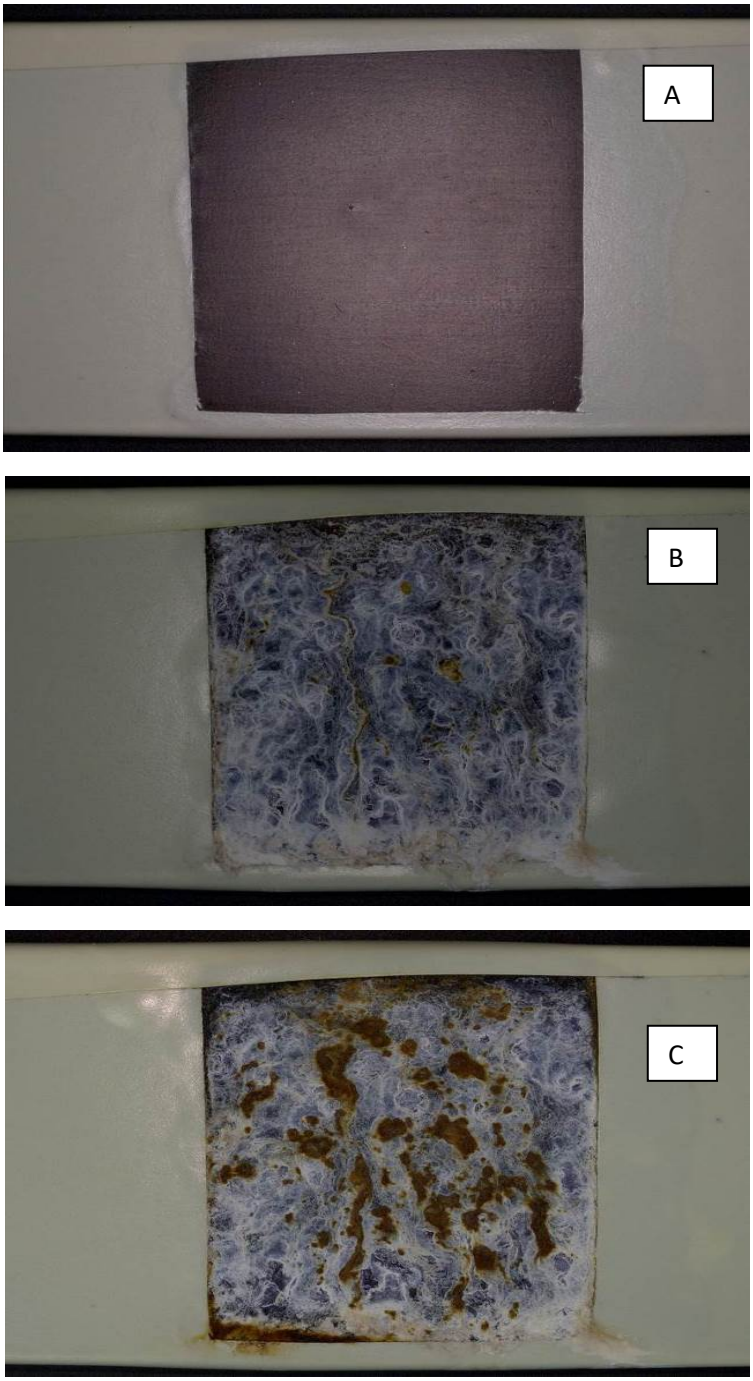

Figure 43. Images of 1L Coating Sample before (A) and NSS Exposure (10 hour (B) and 200 hour (C))

Figure 44. Images of 2L Coating Sample before (A) and after NSS Exposure (200h (B) and 500h (C))

11.2.5. HE Susceptibility Test on 2L CP on Zn-Ni Coated High Strength Steel Coupons Performed at WPAFB/UDRI

The HE susceptibility test was performed according to ASTM F519 method on AISI 4340 steel notched round bars coated with conductive polymer coating. Uncoated bar samples were also tested as controls for the direct comparison of coated vs. uncoated samples. The control standard samples were of the same batch of supplied bars. The test environment was laboratory air at ambient humidity and temperature. As required by ASTM F519, the load force of 75% of NTS was used to assess the brittleness of the rod samples. There were no embrittlement effect (failures) observed during the test as all coated specimens and controls passed the required duration of the load without fracturing (Table 13 and Figure 45). Therefore, the investigated conductive polymer material and the current coating processing can be considered as non-embrittling since no detectable hydrogen embrittlement risk was found by the test defined by ASTM F519.

Table 13. HE Test Results on 2L CP Coated Bars

Coating	Substrate	Environment	%NTS	Embrittling Effect
2L Coating	4340 Steel	Ambient Conditions, Air	75	No
Control (No Coating)	4340 Steel	Ambient Conditions, Air	75	No

Figure 45. Creep Testing Setup; Specimens are loaded vertically in the center of each frame

12.0 Conclusions and Implications for Future Research

Two batches of the newly developed by the NAWCWD conductive polymer coating samples were tested for adhesion (including wet/dry tape adhesion and tensile PATTI adhesion), corrosion resistance properties via a neutral salt spray exposure, and hydrogen embrittlement. In addition to corrosion and adhesion properties testing, the morphology of the coatings was examined by the scanning electron microscopy. Comparative evaluation of coating samples demonstrated reasonably good corrosion performance and strong adhesion to zinc-nickel electroplated steel substrate achieved with the second batch of the coating samples when the coatings were applied in a two-layer fashion for a thicker buildup on Zn-Ni plated high-strength steel substrate. For these two-layer coating samples, the study of the film morphology revealed uniformly dense and defect-free coating, no hydrogen embrittlement during deposition but failure to meet mil spec requirements for contact resistance before and after NSS. The results of testing and the overall improvement in performance achieved starting from the second batch of coating samples brings these coating materials to a promising performance level that would justify further and more detailed investigation of these unique and innovative CP coatings.

13.0 Literature Cited

1. Wilcox G. D. and Gabe D. R., Electrodeposited Zinc Alloy Coatings, *Corrosion Science*, **35**, 1251 (1993).
2. Neacsu E. I., Constatin, V., Soare V., Osiceanu, P., Popa, M. V. and Popecu, A. M. Corrosion Protection of Steel Using ZnNiP Electroless Coatings, *Rev. Chim. (Bucharest)*, **64(9)**, 994 (2013).
3. Lin K. L., Yang C. F., and Lee J. T., Correlation of Microstructure with Corrosion and Electrochemical Behavior of the Batch-type Hot-dip Aluminum-zinc Coatings: Part I. Zinc and 5%Aluminum-zinc Coatings, *Corrosion (Houston, TX, United States)*, **47(1)**, 9 (1991).
4. Thompson M. D., Zinc alloys-The Boeing Alternative to Cadmium, *Trans. Inst. Metal Finish*., **74(3)**, 3 (1996).
5. Shahin, G. E., Decorative Chromium and Cadmium Substitutes, *Proceed. AESF Annual Technical Conference*, **82nd**, 895 (1995).
6. Eliaz N., Venkatakrishna K., and Hedge A. C., Electroplating and Characterization of Zn-Ni, Zn-Co and Zn-Ni-Co Alloys, *Surface Coatings Technology*, **205(7)**, 1969 (2010).
7. Hu C-C., and Wang C-K., Effects of Composition and Reflowing on the Corrosive Behavior of Sn-Zn Deposits in Brine Media, *Electrochimica Acta*, **51(20)**, 4125 (2006).
8. Zhirnov A. D., Karimova S. A., Ovsyannikova L. V., and Gubenko O. A., New Protective Coatings for Replacing Cadmium Coatings on Steel Parts, *Metal Science and Heat Treatment (Translation of Metallovedenie i Termicheskaya Obrabotka Mettallov)*, **45(1-2)**, 23 (2003).
9. Tian W., Xie F. Q., Wu X. Q., and Yang Z. Z., Study on Corrosion Resistance of Electroplating Zinc-Nickel Alloy Coatings, *Surface and Interface Analysis*, **41**, 251 (2009).
10. Siitari D. W., Sagiyama M., and Hara T., Corrosion of Ni-Zn Electrodeposited Alloy, *Transactions of the Iron and Steel Institute of Japan*, **23**, 959 (1983).
11. Trimaran K. R., Brahimi S., Spear J. A., Osborne J. H., and Yue S., Characterization of Corrosion Resistance of Electrodeposited Zn-Ni-Zn and Cd Coatings, *Electrochimica Acta*., **105**, 314 (2013).
12. Abou-Krisha M. M., Assaf F. H., and El-Naby S. A., Electrodeposition and Characterization of Zinc-Nickel-Iron Alloy from Sulfate Bath: Influence of Plating Bath Temperature, *Journal Solid State Electrochemistry*, **13(6)**, 879 (2009).
13. Durairajan, A., Haran B. S., White, R. E. and Popov, B. N., Development of a New Electrodeposition Process for Plating Zn-Ni-X (X = Cd, P) Alloys. Permeation Characteristics of Zn-Ni-Cd Ternary Alloys, *Journal of the Electrochemical Society*, 147(12), 4507 (2000).
14. Durairjan A., Haran B. S., White R. E., Popov B. N., Development of a New Electrodeposition Process for Plating Zn-Ni-X (C= Cd, P) Alloys I. Corrosion Characteristics of Zn-Ni-Cd Ternary Alloys, *Journal of the Electrochemical Society*, **147(5)**, 1781 (2000).

15. Oriquat G. A., Saleem T. H., Naik R. R., Nafady H. A., Abedel A.S. A., Subchronic Toxic Effects of Cadmium in a Rat Model, *Fresenius Environmental Bulletin*, 22(4a), 1054 (2013).
16. Asagba S. O., Comparative Effect of Water and Food-chain Mediated Cadmium Exposure in Rats, *BioMetals*, 23(6), 961 (2010).
17. Ogundele O. M., Sanya J. O., Madukwe J., Caxton-Martins, E. A., Cortical and Cerebellar Neurodegeneration in Cyanide Induced Toxicity, *Journal of Cell and Animal Biology*, 7(3), 31 (2013).
18. Bunke D., and Nakhosteen, C. B., Environmental Issues of Chromium (VI) Compounds, *Journal of Electrochemistry and Plating Technology,* **1(4)**, 12 (2011).
19. Wise S. S., and Wise J. P., Chromium and Genomic Stability, *Mutation Research, Fundamental and Molecular Mechanisms of Mutagenesis*, **733(1-2)**, 78 (2012).
20. Licursi L., and Gomez N., Short-term Toxicity of Hexavalent-Chromium to Epipsammic Diatoms of a Microtidal Estuary (Rio de la Plata): Responses from the Individual Cell to the Community Structure, *Aquatic Toxicity*, 134-135, 83(2013).
21. National Emissions Standards for Chromium Emissions from Hard and Decorative Chromium Electroplating and Chromium Anodizing Tanks, Environmental Protection Agency, Federal Register, RIN 2060-AC14, January 25, 1995
22. AESF/ EPA Conference, Hexavalent Chrome PEL AESF Presentation, January 2004, http://www.nasf.org/nasf-law-regulation.php.
23. Tallman D. E., and Bierwagen, G. P., Corrosion Protection Using Conductive Polymers, In Handbook of Conducting Polymers: Conjugated Polymers: Processing and Applications, Eds. Skotheim, T. A., and Reynolds, J. R., CRC Press, New York, Chapter 15, pp. 15-1-53, 2007.
24. Wessling B., Polymers to Organic Metals, *Chemical Innovation*, January 2001, 35-40.
25. Zarras P., Anderson N., Webber C., Stenger-Smith J. D., Spicer M., and Buhrmaster D. Electroactive Materials as Smart Corrosion-inhibiting Coatings for the Replacement of Hexavalent Chromium, *CoatingsTech*, **8(1)**, 40 (2011).
26. Zarras P., Validation of Novel Electroactive Polymers as Replacement of Hexavalent Chromium Pretreatments, ESTCP WP-200527, Joint Technical Report, in press, 2014.
27. Madden J. D., Polypyrrole Actuators: Properties and Initial Applications, In Electroactive Polymers for Robotics Applications: Artificial Muscles and Sensors, Eds. Kim K. K., and Tadokoro S., Springer-Verlag, London, Chapter 5, pp. 121-152, 2007.
28. Tallman D. E., Spinks G., Dominis A., and Wallace G. G., Electroactive Conducting Polymers for Corrosion Control Part 1: General Introduction and a Review of Nonferrous Metals, *Journal Solid State Electrochemistry*, **6(2)**, 73 (2002).
29. Hua, F., and Ruckelstein E., Copolymers of Aniline and 3-Aminophenol Derivatives with Oligo(oxyethylene) Side Chains as Novel Water-Soluble Conducting Polymers, *Macromolecules*, **37(16)**, 6104 (2004).

30. Goda, T., Toya, M., Matsumoto, A., and Miyahara, Y., Poly(3,4-ethylenedioxythiophene) Bearing Phosphorylcholine groups for Metal-free, Antibody-free, and Low-impedance Biosensors Specific for C-Reactive Protein, *ACS Applied Materials & Interfaces*, **7(49)**, 27440 (2015).
31. Rawal, V. H., Jones, R. J., and Cava, M. P., Photocyclization Strategy for the Synthesis of Anti-tumor Agent CC-1065: Synthesis of the Dideoxy PDE-1 and PDE-II. Synthesis of Thiophene and Furan Analogues of Dideoxy PDE-I and PDE-II, *J. Org. Chem*., **52**, 19 (1987).
32. Ullrich, F. W., and Breitmier E., Vinyl Analogs of the Vilsmeier Formylation with 3-(Dimethylamino) acroleins, *Synthesis*, **8**, 641 (1983).
33. Miller, R. E., and Nord, F.F., Heterocyclics. XV. The Synthesis of Thiophene Polyenes, *J. Org. Chem*., **16**, 1380 (1951).